

Spontaneous Symmetry Breaking in a Shaken and Sheared Granular Flow

Finalized: May 10, 2007

Nicholas Penha Malaya

This research was conducted under the supervision of:
Dr. Jeffrey Urbach and Dr. David Egolf

Submitted in fulfillment of the Senior Thesis requirement
in the Department of Physics, Georgetown University,
Washington, DC, May 2007

Abstract

We show results from a computational simulation of a vibrated granular monolayer inside a three dimensional box. The box is filled with identical particles that are vertically shaken while the walls are moved horizontally to apply shear. As a result, we are able to measure the affect of shear rates largely independent from the thermal temperature. At lower wall speeds we observe a linear velocity profile with some velocity slip at the system boundaries, which implies our granular fluid is consistent, in part, with the Navier-Stokes equation. At a critical velocity gradient the system spontaneously breaks symmetry to a state with a net flow of particles. At even higher wall velocities, we observe a second transition by which the granular media reverts back to a symmetric state, with significant amounts of slip occurring at both walls. The dynamics of the transition appear to be sensitive in part to the wall slip at the boundaries, the velocity profile slope and the system temperature. We also describe the dependence of the instability formation on different system parameters such as density and system size. The transition appears to be consistent with a 2nd order phase transition, and we continue on to discuss our investigations into indications of universality.

Contents

1	An Introduction to Granular Systems	1
2	Our Computational Simulation	5
2.1	General Geometry and Parameters	5
2.2	Force Laws	8
2.3	Implementation	9
2.4	Characteristic Timescales	10
3	Towards a Hydrodynamics of Granular Media	11
3.1	A Hydrodynamic Description	11
3.2	Linear Velocity Profiles	14
3.3	Spontaneous Symmetry Breaking	17
3.4	Density Profiles	21
3.5	Granular Temperature	22
4	The Onset of Instability	25
4.1	System Size and the Instability Formation	25
4.2	A Basic Model	29
4.3	Modifying our Model	33
5	On Continuous Phase Transitions	35
5.1	Introduction	35
5.2	Hysteresis...or the lack thereof	36
5.3	Continuous Bifurcation	38
5.4	Critical Phenomena	42
5.5	Discussion	46
6	Conclusions	48
A	The Experimental Setup	51
B	Comparison with other systems	54

C	Fruitless Pursuits	57
C.1	Mean Free Path	57
C.2	Other Paths Investigated	61
D	The Parameter Space Sampled	63
	References	66
	Acknowledgments	70

Chapter 1

An Introduction to Granular Systems

From the interactions of a rarefied gas to the motion of icebergs or the rings of Saturn, granular systems manifest themselves over a broad range of length scales and contexts.

Granular systems are intriguing in that they can flow like a liquid when shaken and yet hold coherent, if complex, structure when stationary. With such an astounding range of complex behavior, there exists just as broad a range of interest in granular systems ranging from stress chains[1] to avalanches[2]. The emphasis of our research has been on modeling the dynamics of highly energetic, nonequilibrium granular flows.

Granular systems, while often highly nonlinear and still lacking a comprehensive theory, are fundamentally deterministic in nature. By this, we mean these systems do not involve random or noisy inputs. A granular system should obey classical relations, as the characteristic length scales are orders of magnitude larger than those associated with quantum mechanical effects. Any irregular or exceedingly complex behavior exhibited in our system can therefore be attributed to the system's nonlinear or even chaotic effects and not

as some fundamental limit to our knowledge of the system.

The difficulty in accurately modeling granular media stems from a variety of issues. At the forefront is the nonequilibrium environment of our experiment. There is significant dissipation of energy during each granular collision. Due to the fact we are interested in flows, any dynamical system of the granular variety requires constant injections of energy into the system, lest it settle down from the inelastic interactions. A variety of important results of equilibrium statistical mechanics are not applicable because of non-Gaussian velocity distributions, the lack of molecular chaos, and several other factors[3]. Finally, granular systems shun traditional thermodynamic formulations of temperature, which prevents developing a general formula for system-wide fluctuations or the application of the Gibbs distribution.

As a result, the extremely complex behavior exhibited by granular flows can give the appearance of being nearly intractable. It has therefore become common practice to attempt to extend the well understood, powerful results of equilibrium statistical physics to nonequilibrium systems. There exists a multitude of efforts to characterize more complex phenomena with simpler, better understood cases. These works range from statistical descriptions of spatiotemporal chaos[4] to the characterization of nonequilibrium systems that behave like equilibrium systems at coarse grained scales[5]. These successes suggest that while we do not expect to find perfect agreement between our system and classical theories, this can be an effective approach to characterizing our dynamics.

Yet these difficulties also present opportunities. We are in a position to effectively recast statistical mechanics in an entirely new light, which would open up an entire subset

of nature to accurate description. In this paper we will concern ourselves with accurately describing the observed dynamics of a computational simulation of a driven, dissipative granular system that spontaneously breaks symmetry. We will touch upon elements related to a myriad of disciplines in physics from hydrodynamics to statistical mechanics to the nonlinear sciences. As with a variety of other instances in the natural sciences, we find that our system exhibits a variety of conditions that are strikingly 'universal' in nature, and so it is our hope that our research is ultimately beneficial to more than just our specific granular system, but also serves to characterize a broader subset of the universe.

Our approach to this research has been from a computational angle. Physics has increasingly embraced simulation beside experiment and theory, each valued for particular advantages. Our decision to focus on computer simulations stems from the desire to analyze quantities that are prohibitively difficult to measure experimentally. In addition, a computational simulation allows us to quickly adjust any system parameters that might be difficult or expensive to vary, such the Earth's gravitational pull[6]. We have based our simulation on an experimental apparatus from Professor Urbach's lab. Experiments have been performed on this set-up and are the subject of Appendix A, but in general this report is concerned with the results from a computational simulation of a granular system.

The goal of our work is twofold. We seek to accurately describe the dynamics of granular flows. We are investigating the accuracy of modeling our granular system with equations more common to fluid dynamics. Continuing this reasoning, we are attempting to model the formation of an asymmetric state as a hydrodynamic instability. In addition, we have probed the dynamics of the symmetry breaking, and have applied tools and methods com-

mon to statistical mechanics in order to more accurately characterize the transition to an asymmetric state.

Chapter 2

Our Computational Simulation

2.1 General Geometry and Parameters

As stated previously, all of our data has come from computer simulations conducted using a program we have developed using techniques similar to previous granular simulations[7].

Our computational simulation is a vibrated granular monolayer inside a three dimensional box. A typical state is seen in Fig. 2.1. A monolayer is formed because the distance between vertical plates is 1.7 ball diameters. As a result, our system is quasi two-dimensional in that our balls cannot bounce over each other. The box is filled with identical particles that are vertically shaken while the opposing horizontal walls are moved in opposite directions to apply shear. Finally, there are periodic boundary conditions in the y-direction, so as to linearly approximate the circular experimental apparatus. For more on the experimental apparatus that this model is based on, see Appendix A.

Our shearing walls (see Fig. 2.1 highlighted in red and blue) are composed of rigid balls

‘glued’ together.

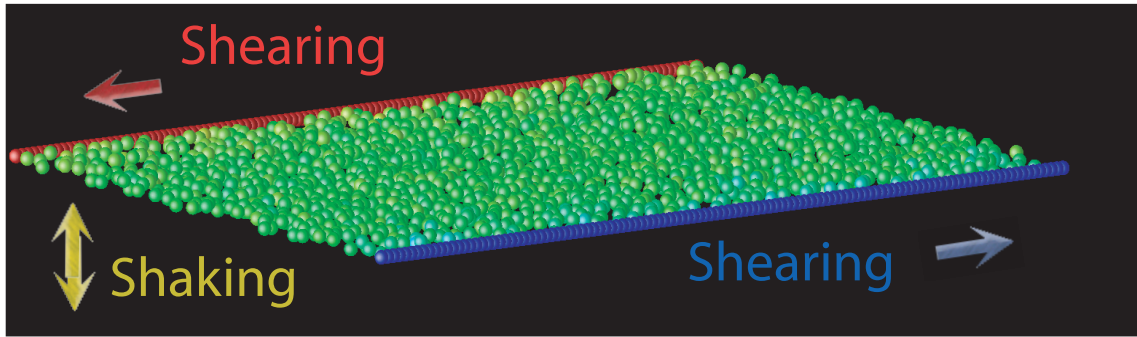


Figure 2.1: A skew view of our simulation

From this picture you can clearly see the wall balls. The distance between the two walls is L_x (generally referred to as the system width), and the length of the walls is defined as L_y . We calculate these lengths from the system density d , and the number of particles N , from which we determine a hexagonal packing density:

$$L_y = 2\sqrt{3} + 2\sqrt{3}\sqrt{\left(1 + \frac{2N}{d\sqrt{3}}\right)}$$

$$L_x = \frac{2\sqrt{3}NR^2}{d(L_y - R\sqrt{3})}$$

Note that because of how we construct our walls, L_y must be an integer.

A typical simulation has approximately 2000 spheres, a density of about .5, a width (L_x) of approximately 59 ball diameters, and a length (L_y) of around 234 spheres. As stated previously, collisions are inelastic, and so a driving force is necessary to keep the system ‘going’. In our system, this takes the form of the shaking plates. The amplitude

of shaking is generally about .25 ball radii, with a peak speed of 3 ball radii per shaking period. The wall speeds range anywhere from 30 ball radii per period to 90 ball radii per period. This is a total velocity difference between the shearing walls, which means that should the system be running with a velocity of 30, each wall is moving at 15 ball radii per period in opposite directions. For more on the parameter space over which the system has been run, see Appendix D.

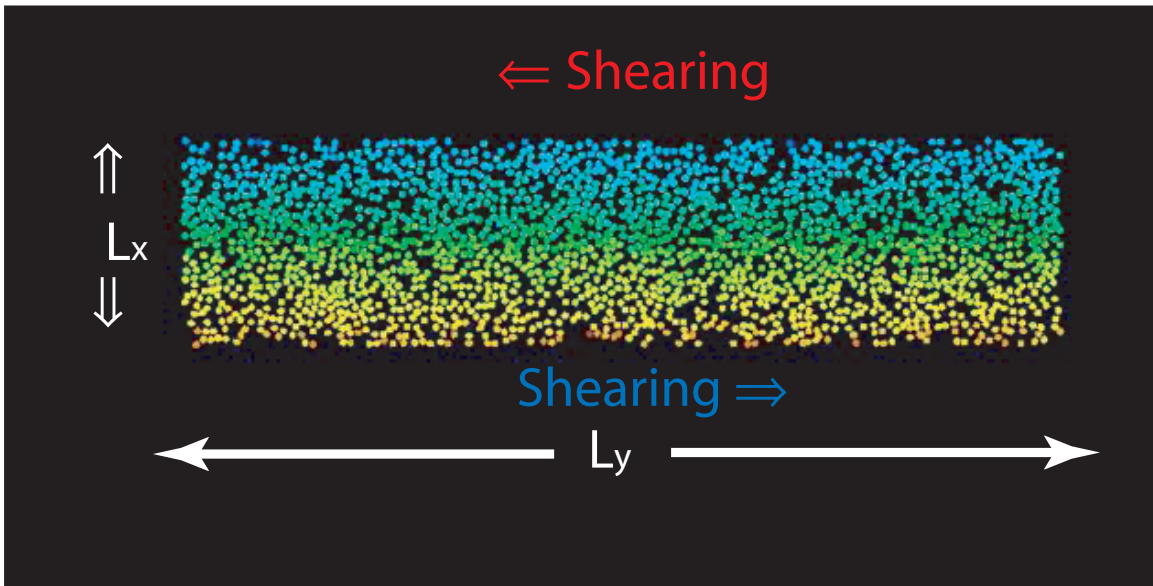


Figure 2.2: A view from above

In Fig. 2.2, the spheres are color coded to demonstrate the range of velocities in the system, implying a relatively uniform velocity gradient between the opposing plates shear directions.

As stated in the introduction, granular systems exhibit deterministic behavior. As a result, it would be inappropriate to introduce randomness into our simulation and expect our model to provide a complete description of the dynamics of granular flows. Concordantly,

the Gear predictor-corrector method, the force laws and all the dynamics of our system have no random terms. The only stochastic implementation of our program occurs when generating the initial positions of the particles. Therefore, we can be confident that the phenomena we are examining are completely deterministic because any simulation initialized with the same random parameters and initial seed will have totally identical behavior.

2.2 Force Laws

Interactions between particles and the walls are dictated by three separate forces. For any given interaction there will be:

A repulsive spring force:

$$F_n^{\text{spring}} = k\delta$$

A dissipative force during collisions:

$$F_n^{\text{dissipation}} = \gamma_n \delta_n$$

Finally, a tangential frictional force:

$$F_n^{\text{friction}} = \gamma_s \delta_t$$

Here, k is a spring constant between particles and γ_n and γ_s are coefficients of normal restitution and friction, respectively. δ represents the overlap between particles, and as such, must be less than zero. These Forces are integrated numerically using a Gear predictor-corrector scheme to determine new positions and velocities. Readers interested in the specifics of its implementation should see Ref. [8].

In Fig. 2.3 below, you can see the forces between two particles.

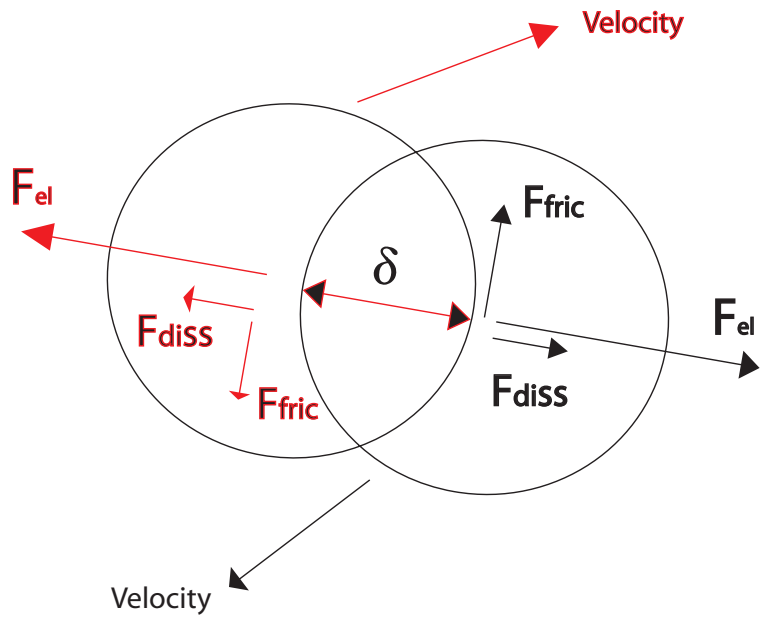


Figure 2.3: A typical interaction in our system.

2.3 Implementation

All of the data from these simulations was created from runs using the same basic code, with modifications only to the data to be outputted and the input parameters. The runs were conducted on *Melvin*, which is made up of 48 Apple G4 processors, and *Fire*, an 20 node G5 cluster. Our program was implemented in an embarrassingly parallel format in C, with data analysis performed in Data Explorer. The average simulation runtime was several hours.

In general, our results are statistical in nature we are taking ensemble averages of our runs. In order to fully minimize the effect of fluctuations or other statistically issues in individual system runs, our data is actually the average of several simulations all initialized with identical system parameters and different initial conditions, which should serve to

thoroughly smooth out our data and ensure our results are statistically valid.

2.4 Characteristic Timescales

In general it is useful to discuss theoretical models in dimensionless terms. The principle utility of nondimensionalization comes from simplifying our discussion to only quantities intrinsic to our system. By putting our system in dimensionless form, we are effectively replacing SI units with quantities that are proportional to the natural scaling of our system. Finally, it is especially useful to examine our granular system with dimensionless quantities, as granular systems are particularly applicable to a wide range of length scales.

Our system possesses several characteristic scales that are worthy of mention at this time. The natural length scale of our system is clearly set by the ball diameter of our particles. Our characteristic timescale is less obvious. We expect that the period of oscillation of the shaking plate dictates the intermolecular collision times, as this is fundamentally setting the energy of our particles. This is because basic kinetic theory, which we expect to hold in this case, predicts the intermolecular collision times to scale with the square root of the temperature[9].

As a result, for the discussion and graphs of this report, we will be using these ‘natural’ system units. Lengths will be in ball radii, and timescales in units of plate oscillation periods.

Chapter 3

Towards a Hydrodynamics of Granular Media

3.1 A Hydrodynamic Description

An important question specific to granular systems relates to accuracy of modeling a discrete system with equations more commonly associated with continuous hydrodynamic equations. Several factors lead us to believe that our granular system can be accurately described in such a manner. Specifically, our basis for this statement is prompted by observations of linear velocity profiles as well as the direct proportionality between system width and the critical wall speed.

A reasonable starting point for quantitatively describing the dynamics of a fluid is provided by the Navier-Stokes equations. It is generally believed that the Navier-Stokes equations provide the most complete picture of bulk fluid dynamics, as they are differential

equations derived from Newtonian mechanics that describe the rates of flux of the variables of interest[10]. While this implies they accurately describe a fluid, the equations themselves seriously resist analytical solutions for all but the simplest conditions, and so are usually approached numerically. Nonetheless, our basic granular flow is sufficiently uncomplicated so as to lend itself, at least initially, to an effective description from this perspective. A derivation of the Navier-Stokes is unnecessary for our purposes, so we will begin with it *a priori*[11].

We therefore start with:

$$\frac{\partial \vec{V}}{\partial t} + \vec{V} \vec{\nabla} \vec{V} = -\frac{\vec{\nabla} P}{\rho} + \nu \nabla^2 \vec{V} + \frac{\vec{F}}{\rho},$$

where

$$\nu = \frac{\mu}{\rho}$$

is defined as the kinematic viscosity.

In this nonlinear partial differential equation (the Navier-Stokes), μ is the coefficient of viscosity, ρ the density, \vec{V} the velocity vector and P the pressure. \vec{F} represents the body forces. In all our considerations, the net force will be zero, and so the \vec{F} term drops out.

If we assume that our system is in steady state $\frac{\partial \vec{V}}{\partial t} = 0$ (an assumption I will attempt to prompt with data at a later time), and has a negligible pressure gradient $\vec{\nabla} P = 0$. We can significantly simplify our equation yielding,

$$\nu \nabla^2 \vec{V} = 0,$$

Because our system is periodic in the x-direction,

$$\nu \frac{\partial^2 V_y}{\partial x^2} = 0.$$

This solution corresponds to linear velocity profiles over the x-direction, i.e. between shearing walls. (This assumes friction is not significant or completely absent, See appendix A for more.) Therefore, if these assumptions hold, we expect that our simulation will have linear velocity profiles across the width of the cell. An example of what this would look like is below (note that the position is in terms of Lx).

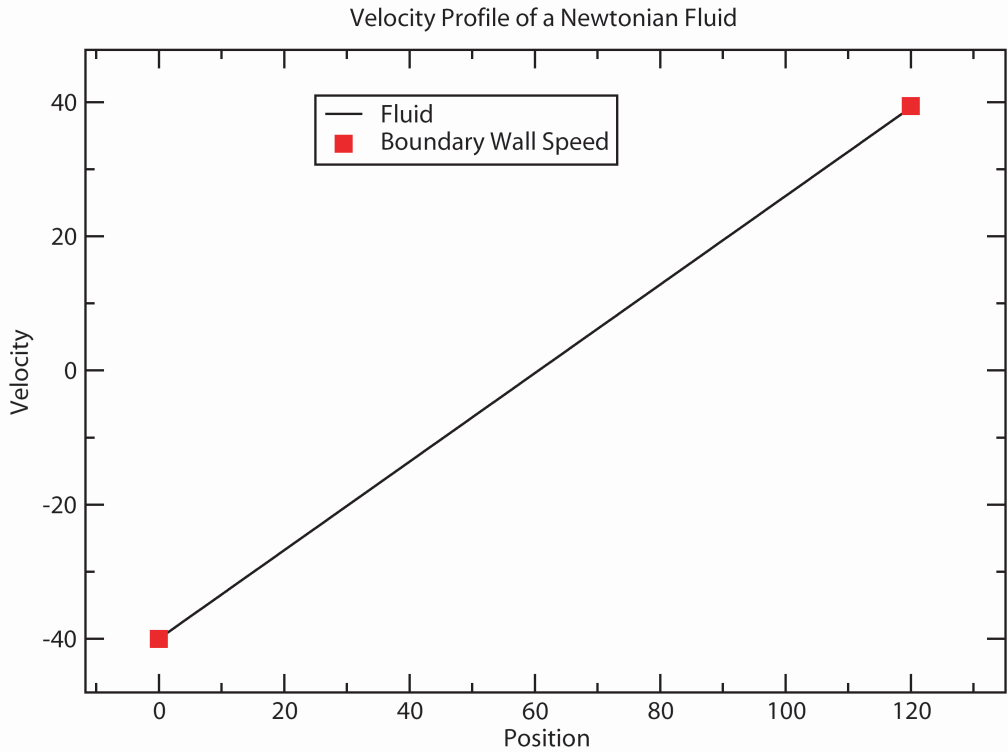


Figure 3.1: A linear velocity profile for a newtonian fluid

At this time, it is important to note that there are several significant assumptions underlying this result. By starting with the Navier-Stokes, we are implicitly assuming our granular flow will behave like a Newtonian Fluid. This is a potentially flawed assumption,

as our granular flow is without question compressible, for as we shall observe later, the density of our flows is neither constant nor uniform. It would perhaps be more appropriate to treat our fluid as a rarefied gas flow (see Appendix C) as we expect that the granular system will not obey the ‘no-slip’ condition[12] as with a continuous medium. Nevertheless, it is useful to prompt our thinking on granular flows with comparisons to simple fluids.

3.2 Linear Velocity Profiles

In Fig. 3.2 you can see our system does have linear velocity profiles. Notice, however, that the system does not have linear velocity profiles over the full range of the width of the system. There exist small ‘layers’ between the walls and bulk granular fluid which do not conform to our most basic hydrodynamic model. We currently believe that these layers may be analogous to the Knudson layers that form in rarefied gases[13]. We will provide a more complete description of the dynamics of these layers in Section 4.

This graph depicts the linear velocity profile formed with a gradient of velocity between shearing walls of 30 ball radii per period of oscillation of the shaken bottom plate. In practice, this means each wall is moving at 15 ball radii per period of oscillation in opposite directions. With regards to the data collection that underlies these profiles, our procedure is to average the results of a large number of snapshots (generally about 8,000 at different times), with the individual particle velocities from each frame being stored in a set of ‘bins’ that are then averaged over the number of particles and frames to yield an average speed within that strip along the x-direction. In the subsequent graphs the individual bins are not

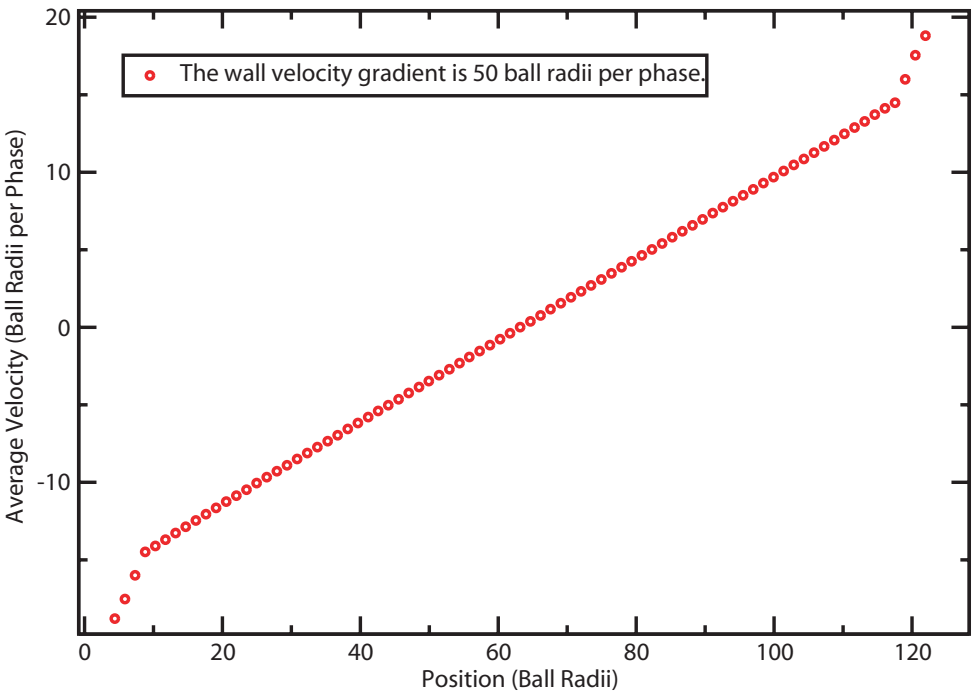


Figure 3.2: A linear velocity profile, where position is the distance between shearing walls (L_x)

drawn continuously so as to demonstrate the discrete nature of the data collection. Readers curious about the instantaneous velocity distributions can find more in Ref. [14].

It is also important to note that we have done tests to assess the validity of our methodology, by observing the number of frames necessary to average over to produce linear velocity profiles. Additionally, we must be careful to ensure that the linear profiles generated are not varying in time. We have done this by examining profiles averaged over a range of different frame counts. As you can see, several thousand frames are more than enough to

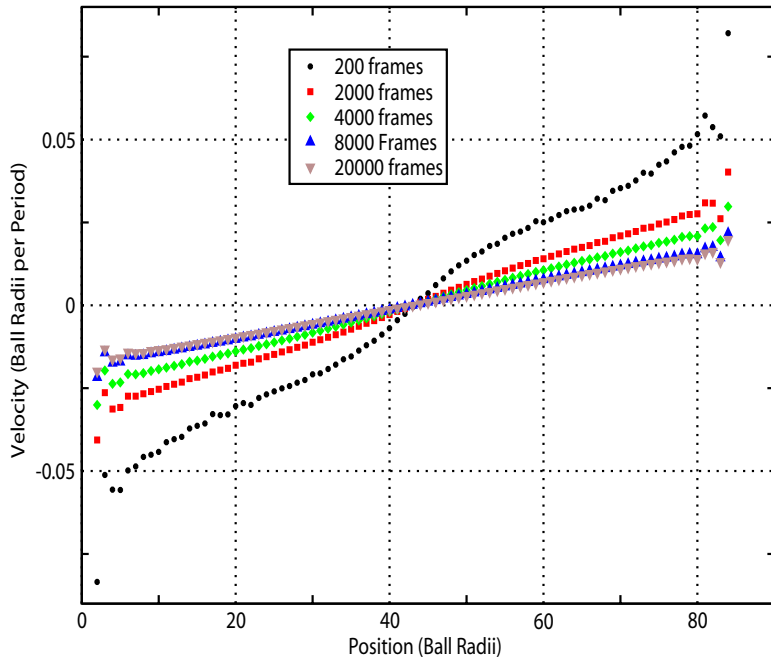


Figure 3.3: Velocity profile averaged over different frame counts. We find effectively no change between 8000 and 20000 frames

accurately describe a linear system profile, and this will not change with increasing frame counts. The result is that we are confident that averaging over this number of frames will give us a statistically valid description of our system. Additionally, this can be regarded as verification that our earlier assumption about the steady state condition of the system was correct.

3.3 Spontaneous Symmetry Breaking

As stated previously, our system is not as simple as our initial, naive viewpoint would suggest. In fact, we have observed that for certain conditions our system undergoes a unique transition to a more complex, asymmetric state. Specifically, we observe that for some range of values for shearing wall velocities, the system is driven out of a symmetric profile, with asymmetries manifesting in the velocity profiles, density profiles, temperature graphs and a variety of other parameters.

The physics underlying the transition is not yet well known, and has been the primary point of interest for this study. Continuing with our interest in modeling this granular flow from a purely hydrodynamic perspective, we have investigated the possibility that this symmetry breaking shares similarities with Couette flows or is analogous in some way to another fluid instability.

Before the onset of the instability, we observe that the velocity profile of the bulk of our granular fluid becomes steeper at higher wall velocities. (Fig. 3.4) The graph depicts the velocity over the range of the system width (position between shearing walls). This forms part of the basis for our basic hypothesis about the symmetry breaking in the system, namely, that there exists a maximum shear within our system, and any attempt to increase the shear (by increasing the wall speed, etc.) will drive the system out of the symmetric state. Below you can see a graph for several velocities within the symmetric regime of our system. Here, increases in wall shear rates increase the velocity profile gradient. You can clearly see that each state is symmetric from the fact that the velocity profile is odd about

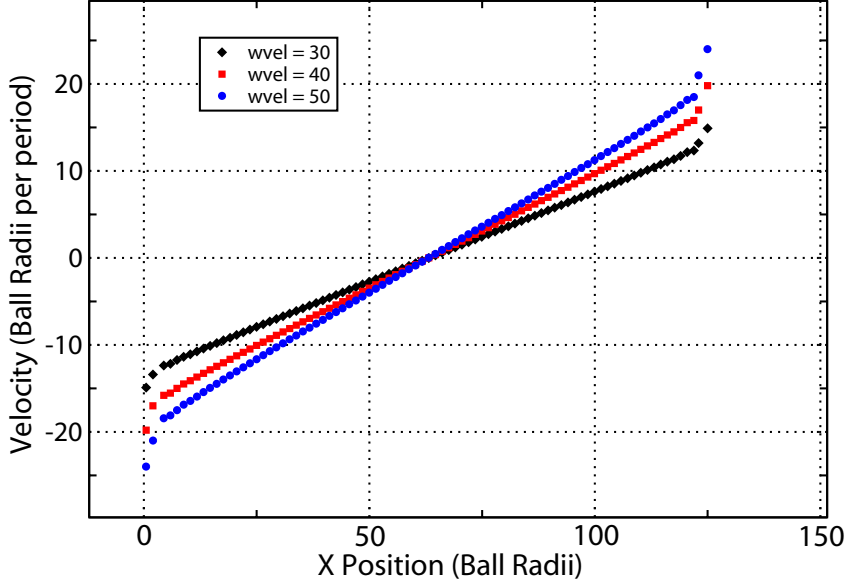


Figure 3.4: Notice that the slope increases for higher wall speeds

the middle of the system.

Fig. 3.5 shows velocity profiles for a range of asymmetric states. The slope of the velocity profile remains relatively constant. Instead, the system appears to account for the increased shear rates between the opposing walls. This leads to a larger mean system speed at higher shear rates over the range of the unstable regime. (See section 4 for a more quantitative discussion of this.) It is important to note that as the system is driven from the symmetric state, the ‘wall slip’ or difference between the bulk velocity at the boundaries and the velocity of the shearing walls is found to increase substantially for one wall. Our explanation of this increase in the wall slip in the asymmetric state is that because the system has attempted to surpass the maximum allowed slope gradient, one wall

Comparison between Symmetric and Asymmetric Velocity Profile

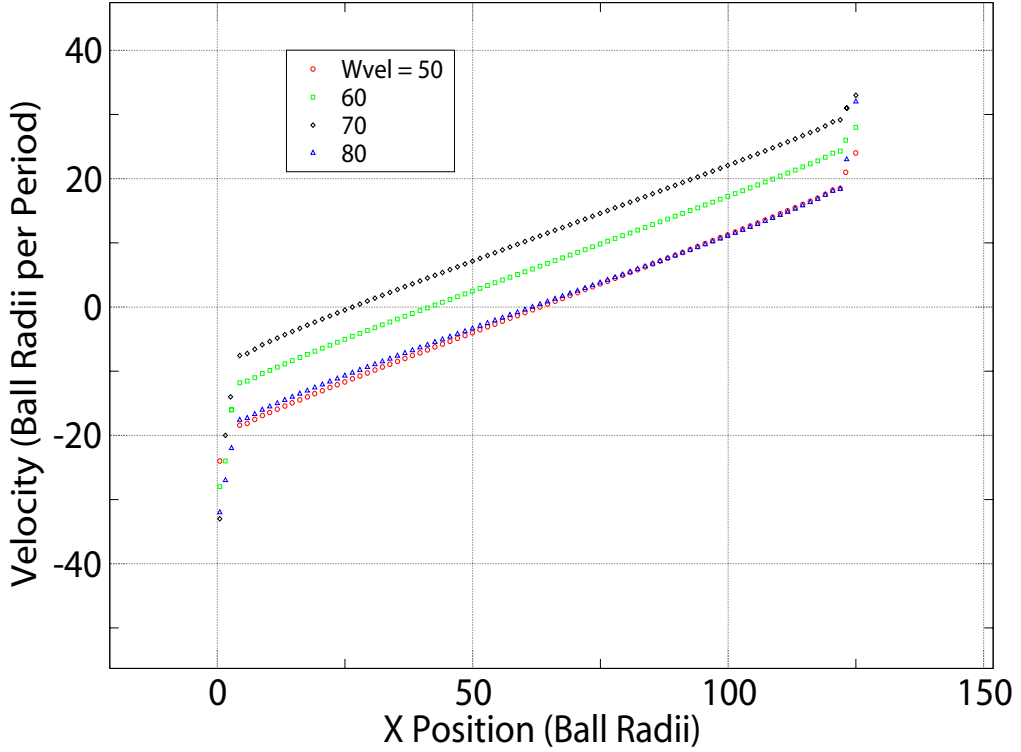


Figure 3.5: The system increasingly breaks symmetry.

spontaneously begins to slip. At this point, the system is driven from its equilibrium state by the other wall which has not yet begun to slip. This provides a possible description of the system's 2nd transition back to the symmetric state at high velocities. Specifically, we believe that the system cannot maintain the increasing wall velocity profiles even within the asymmetric state (i.e., with one wall already slipping), and so both walls begin to slip greatly, and the bulk fluid moves back to a symmetric state.

In addition, we feel compelled to briefly discuss the frequency of symmetry breaking,

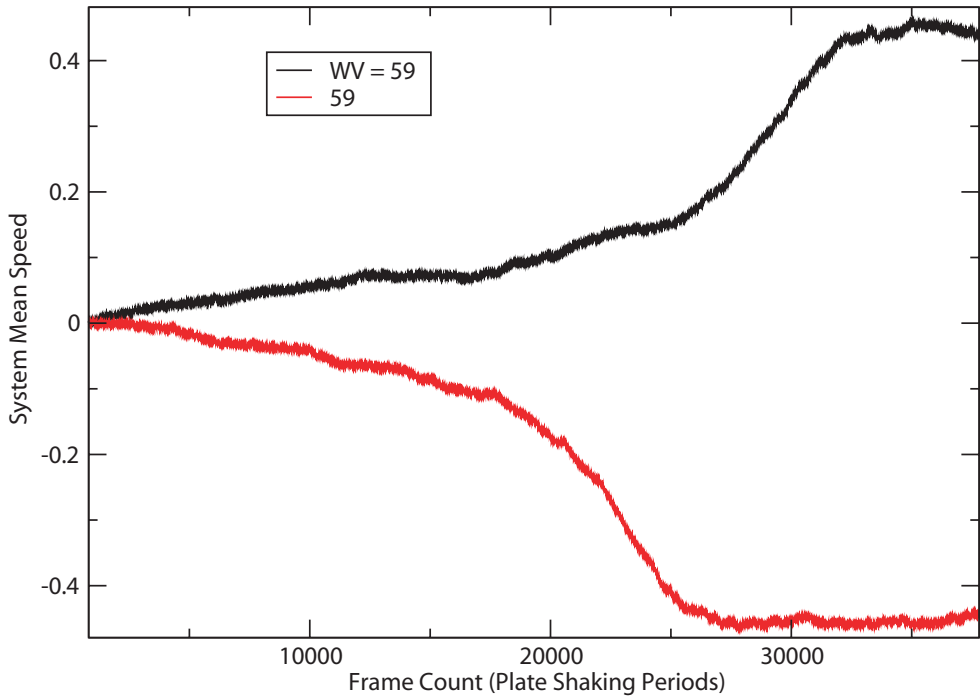


Figure 3.6: Our system has positive and negative asymmetric velocity profiles.

in particular the symmetry between the system evolving to a positive mean speed and a negative one. (See Fig. 3.6.) The graph above provides an excellent example of the two asymmetric states our system can evolve to. These each correspond to a different wall beginning to slip, which drives the system out of a symmetric state. Notice also that for any given run we see significant fluctuations between the time to reach steady state, as well as the particular path followed to this state. However, the final state will always be the same, with the sign of the system mean speed only corresponding to the direction of the flow. Additionally, we have found that the system splits equally between positive and

negative mean speeds. This is expected since our system geometry is perfectly symmetric, and so there should be no ‘preferred’ direction.

For the graphs presented in this report, we will be presenting data that exclusively appears to have broken symmetry to a positive mean speed. We are actually using the absolute values because it is often most useful to compare datasets that have broken symmetry in the same direction, and should not be construed as a lack of an equal quantity of splitting directions between positive and negative velocity profiles.

3.4 Density Profiles

The velocity profiles shown are certainly not intended to present the complete picture of the system dynamics over the transition. The instability formation is far richer and more complex than merely a bifurcation in the velocity profile. Indeed, we observe interesting symmetry breaking in a variety of quantities. For completeness sake, we present some of these different profiles for the symmetric and asymmetric regimes.

The density profiles, seen above in Fig. 3.7, demonstrate the asymmetries that occur when one wall begins to slip. Notice that the symmetric profile breaks symmetry after the critical point, and then regains symmetry after the 2nd transition. The symmetry breaking is manifest mostly not in the bulk of the fluid, but in density changes on the edges. This suggests that the transition is a local phenomenon, as the dynamics do not change towards the middle of the cell, but only at the layers. Finally, it is important to note that the layers have strange density peaks at some distance away from the shearing wall. The reason for

Density Profiles

For symmetric (blue), asymmetric (black) and double slip (red) state

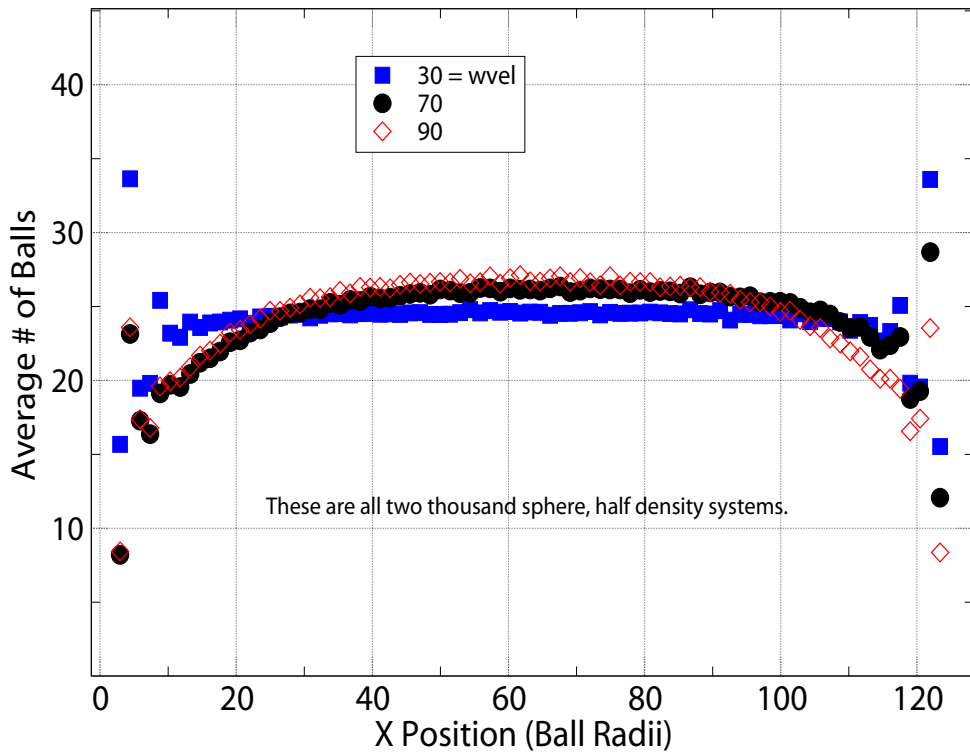


Figure 3.7: Symmetric, Asymmetric and Symmetric (after 2nd transition) density profiles

this is not currently well understood, but it appears that the density peaks near the edges are not sensitive to the binning size used; i.e. they correspond to actual physics and are not simply a computational anomaly.

3.5 Granular Temperature

One of the most ubiquitous classical thermodynamic quantities is temperature. In general a granular system defies conventional classical thermodynamic metrics. It is common to

characterize granular flows with a unique definition of ‘granular temperature’, which is the velocity variance as a function of position:

$$T = \langle (V - \langle V \rangle)^2 \rangle$$

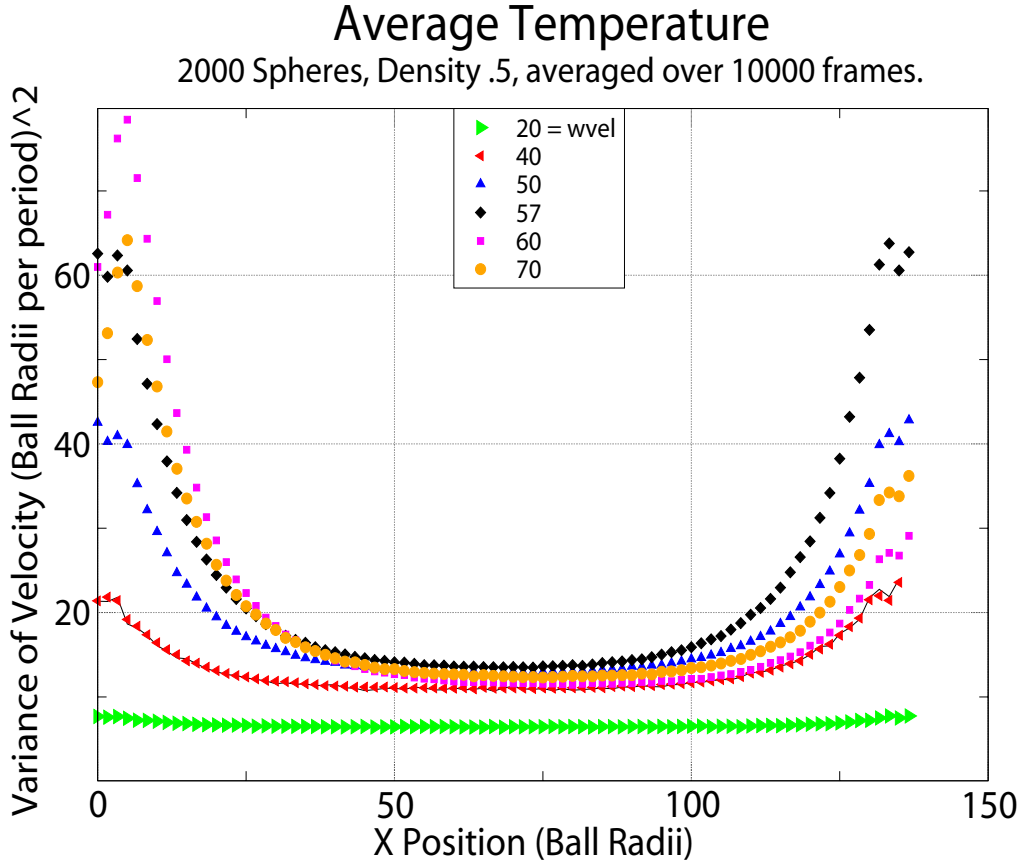


Figure 3.8: Temperature greatly rises at the shearing walls.

Our temperature is therefore a function of the local velocity and is proportional to the kinetic energy. In Fig. 3.8, you can see typical graphs of the average temperature as a function of position between shearing plates. Notice that the boundary layers are again visible.

In other shear experiments, the only influx of energy to the granular system is from the shearing walls. This results in a highly non-uniform temperature over the length of the cell, as well as coupling the shear and system energy together. Our experiment decouples these parameters through the addition of shaking, and this has allowed us to more clearly examine the relationship between the shearing walls and the bulk system dynamics. As can be seen in Fig. 3.8, the lower shearing velocity simulations have an almost uniform temperature between the shearing plates. At higher shear rates, the temperature increase near the walls becomes significantly larger than the bulk, and this implies that there is a wider range of particle velocities near the edges. In addition, it is important to note that the temperature graphs also break symmetry at the formation of the instability, with the system temperature lower at the wall that has larger slip.

Chapter 4

The Onset of Instability

4.1 System Size and the Instability Formation

Several times we have discussed our basic hypothesis about the symmetry breaking in our system. This is that the instability formation we observe in our system can be accurately described by exceeding some critical shear rate which spontaneously causes one of the walls to increase in slip and dictates the evolution of the velocity profile away from a symmetric state. In this section we will discuss the empirical data that we have gathered and how it appears to support this hypothesis. We will derive a simple relation between the shear profile slope, slip and relate this to the intercept of the critical wall speed.

Within hydrodynamic systems, we expect that any accurate description of the dynamics of the system will be dictated by the local interactions between particles, given that ultimately the only driving mechanism of any activity is the interaction between these particles. From this perspective, our critical velocity profile hypothesis can be described as

the maximum local velocity difference between particles. As any individual particle will not possess any information about the system outside of its immediate area, and because of the relative homogeneity of the distribution of particle speeds within a local region, the only 'information' any given particle possesses with regards to the local velocity profile is the relative velocity of particles nearby; clearly from its reference frame it has no idea how quickly it is going. This naturally leads us to believe that a fundamental parameter to look at is the rate of change in velocity for particles near each other, i.e. the slope of the velocity profile. Additionally, it provides perspective into the onset of instability, namely that the system is unable to sustain some local distribution of particle speeds.

If our granular system is in fact acting in a manner consistent with a simple hydrodynamic fluid, we would expect that the onset of the instability would be directly proportional to the width of the system, as shown in Fig. 4.1. For a liquid, we expect the 'no-slip' condition to hold. That is to say, the fluid's velocity profile would continuously map between the wall velocities of the shearing plates. At the boundary between the fluid and the edges, the fluid would have the same velocity as the driving wall, zero speed at the middle of the cell, and would match the speed of the opposite wall at the other side. While the presence of boundary layers implies our system does not perfectly match this typical hydrodynamic model, it approximately does over the symmetric range of wall velocities, with the linear velocity profile increasing for higher wall velocities. This clearly breaks down when our system enters the asymmetric state, as the wall slip increases substantially in this region.

Finally, we can discuss our reasoning behind our expectation of the direct proportionality between the critical wall velocity and the system width. We will return to our locality

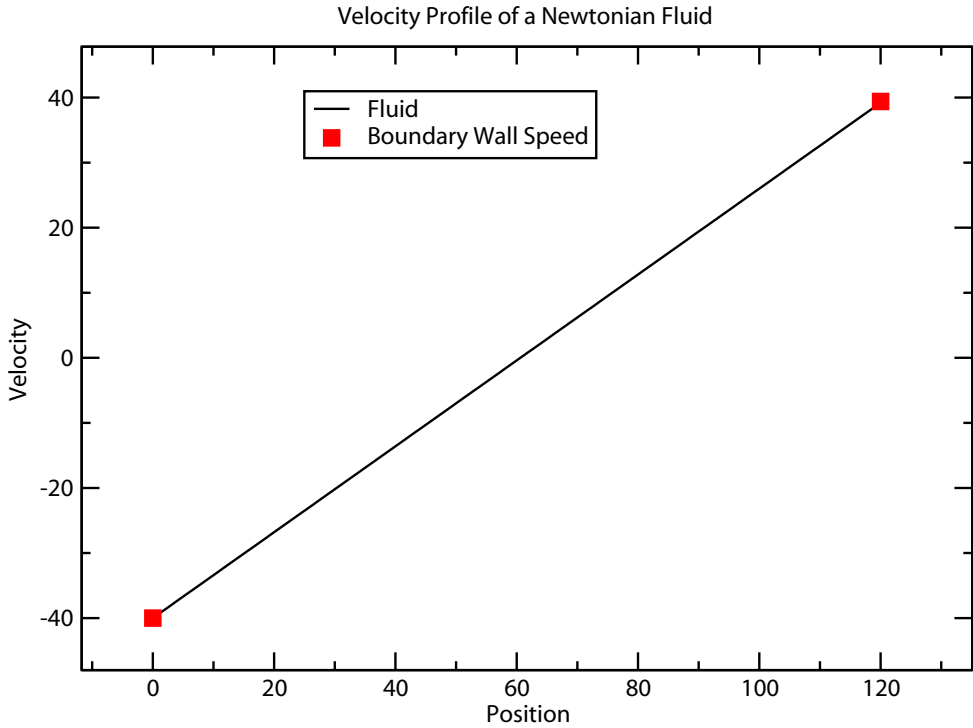


Figure 4.1: Velocity linearly increases with increases in system width for a newtonian fluid.

arguments stated previously, in that a particle has no knowledge of its own velocity outside of the local speed of nearby particles. From this perspective, there is no microscopic difference between the activities of the particles at any position in our system in the region obeying the linear velocity profile. An observer ‘riding along’ with any given particle not on the boundary of the system would have no way of finding his position inside the system. Therefore, we should expect no fundamental change in the dynamics of our system should we increase the width of the system. Our granular spheres would still form a linear velocity profile and would break symmetry at some critical value of slope that locally the particles

could not maintain. Therefore, we can state that we would expect a proportional increase in the critical wall speed for an increase in system width. Indeed, this is what we have observed over a wide range of system sizes, as shown in (Fig. 4.2).

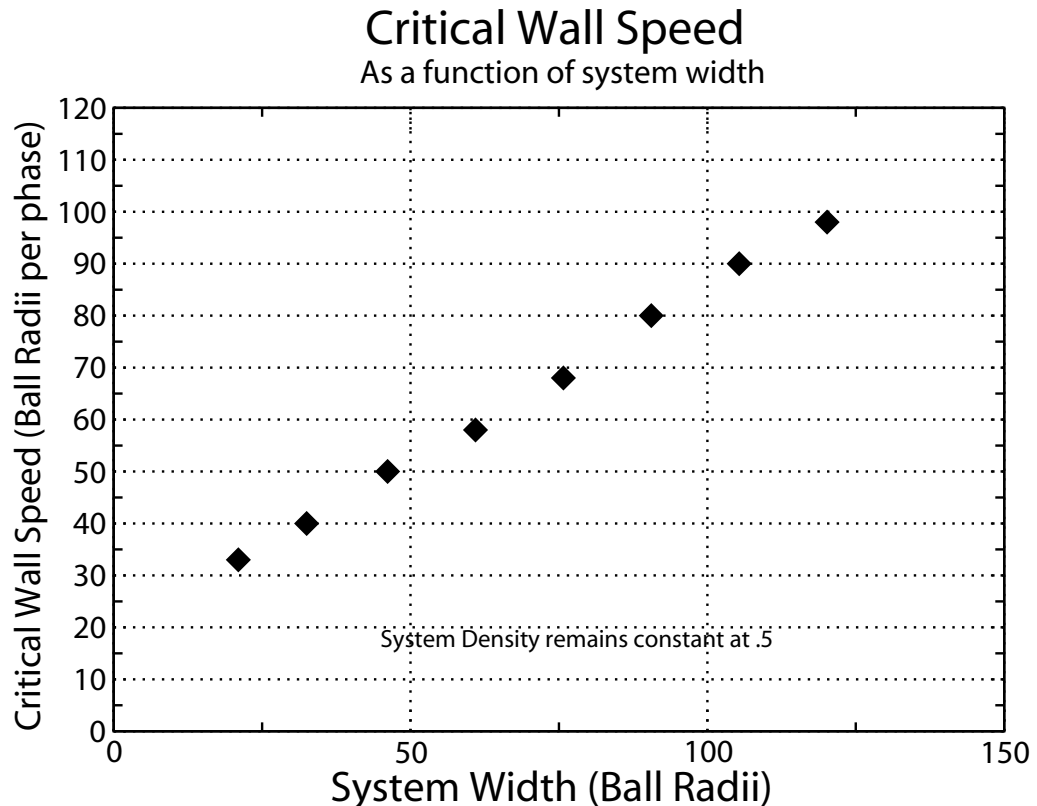


Figure 4.2: Critical Wall Speed and System Width are Directly Proportional

Notice however, that in this graph, the intercept does not go through zero. In fact, we find that the system appears to have a non-zero critical wall speed even at quite small system widths. This intercept occurs at approximately 20 ball radii per period. A possible explanation of this intercept is discussed in Section 4.2. In addition, the slope of our graph is not equal to unity. We will refer to this slope as C, and find it to be approximately .66 for

our most basic system. It has units of inverse oscillation periods.

Just as we were interested in the relationship between the distance between the shearing plates and the critical speed necessary to form an instability, so too did we experiment with changes to the length of the system and the effect that would have on the symmetry breaking in our system. We find that the wall velocity necessary to cause the system to form an instability is independent of the length of the system. In other words, making the system longer while holding the distance between shearing plates constant would not affect the speed needed to break the symmetry of the simulation. We would expect this because any position along the L_x direction, the particle will be exposed to the same amount of shear from the walls.

4.2 A Basic Model

As we discussed previously, it appears anomalous that the critical wall speed would not go to zero as the system width was brought to zero. Furthermore, this wall speed intercept is far from negligible, as it is approximately 22 ball radii per period. Some of this is quite possibly due to our calculation of the system width[21].

Perhaps our most basic hypothesis of the system is that it can only maintain some critical velocity gradient (manifest most clearly as a maximal linear velocity profile over the position between shearing walls) before one wall begins to slip and in doing so, breaks the symmetry of our system. We therefore have focused much of our efforts on creating an effective phenomenology that could predict the basic form of our system parameters.

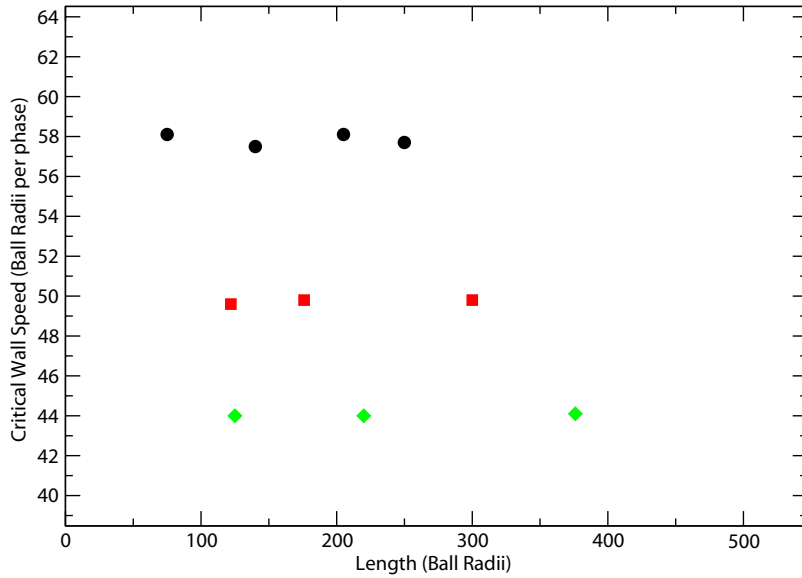


Figure 4.3: In the figure above, you can see that for some given L_x (60, 50 and 40 are shown) the wall speed necessary to cause a transition to an asymmetric state remains unchanged for a wide range of lengths.

A successful ‘toy model’ would, in our eyes, predict the linear velocity profile slope and boundary layer size leading up to the instability, as well as predicting the particular wall velocity at which the system will break symmetry. Our results have certainly been successful, if not completely so, and as is common with problems in scientific research, have lead to just as many questions as answers.

We prompted our most basic model with the simplest relationship we could expect between three important parameters: our velocity profile slope C and the speed of the

shearing walls V_c :

$$V_c = CL_x + V_0$$

where L_x is the width between shearing plates, and V_0 is the intercept which we expect to be related to the velocity slip at the walls (with units of ball radii per oscillation period).

Likewise, from our linear velocity profile, we say that the velocity at any point between shearing walls, $V(x)$, can be defined as:

$$V(x) = \gamma_c x - q$$

Here, γ_c is the slope of the linear velocity profile (units of inverse shaking oscillation periods), x is the position in the cell (ball radii), and q represents the total velocity slip at the walls (ball radii per oscillation period).

Clearly, we are interested in the relationship between C and γ_c as well as V_0 and q . We can expect there to be some sort of relation between these quantities because they all hold the same dimensional units, and, as we will discuss shortly, are similar in magnitude. Additionally, knowing that the critical wall speed varied linearly with the change in system width, it is relatively intuitive to propose that the critical system velocity slope must have something in common with the linear velocity profiles we observe in our fluid. We therefore expect that our γ_c will be approximately equal to C .

If you will remember, V_0 is the intercept of the wall velocity necessary to break symmetry in any system. It is possible that for systems with little room between shearing plates, there will be no region of bulk granular flow, but instead the entire region will be comprised of the boundary layer flow. If this were the case, then we would expect the V_0 to be similar

to our value of q , since it is only when the system is larger than the size of the boundary layers that it will have a region of flow that might be capable of forming linear velocity profiles, and with that, breaking symmetry. From the most basic perspective, our reasoning appears to be on track because we do find that this theoretical model has similarities to the actual fluid, as seen in (Fig. 4.4).

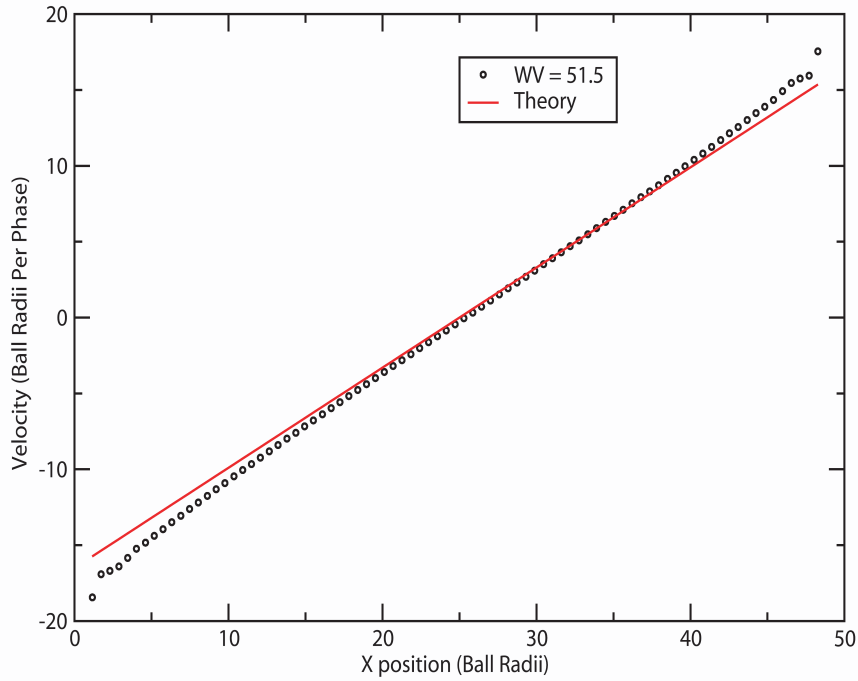


Figure 4.4: Velocity Profile Comparison to Toy Model

However, a comparison between the black line (the actual data) and our red line (the toy model) shows that our guess is not entirely correct. In particular, the slope we used (γ_c) holds a value of approximately .66 ball radii per period, when the slope of our velocity profile is closer to .73 ball radii per period. This difference of approximately 10% implies we do not have a complete picture, and so we looked to modify our theory to more accurately

describe the system. In fact, the blue line on Fig. 4.4 shows our toy model with a $\gamma_c = .73$ ball radii per phase, implying that if we could account for the different slopes, we would have a highly accurate model. We therefore sought to compile a wide range of γ_c 's and q 's for a large section of the parameter space, with the hopes of casting some light onto what precisely was causing our model to break down.

4.3 Modifying our Model

We are forced to adopt the belief that our most primitive model for the granular behavior requires modification. Perhaps the simplest model we could adopt that modifies the slope appropriately would be to add a dependence on wall speed to the boundary layer q . This could take a form such as:

$$V(x) = \gamma_c x - q(V_{\text{wall}})$$

which would require that q now have units of inverse oscillation periods.

In order to accurately probe the relation of q to our wall velocity, we measure a variety of values for q leading up to the instability. (Fig. 4.5) However, we additionally note that the slope of the velocity profiles is no always at a value of .73. Therefore, we looked at several different frequencies of oscillation.

Several elements of the graph are relatively intuitive. Independent of the shaking frequency, the system appears to have a linear increase in the boundary layer size as you increase the shearing wall velocity. This stops when the system approaches the instability, where the system ‘sticks’ near the symmetry breaking.

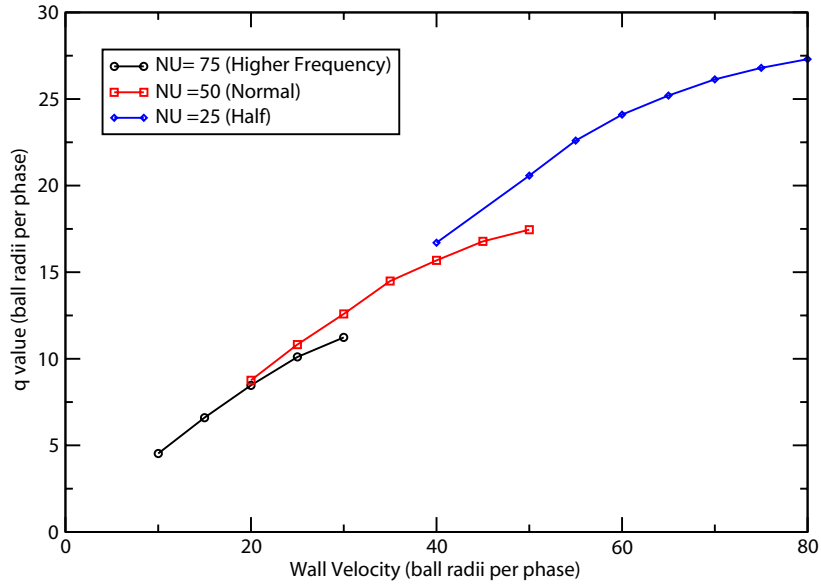


Figure 4.5: q as a function of wall velocity, for a range of frequencies

Unfortunately, our efforts at this point became sidelined by the fact that the relationship between wall velocity and q is complex near the instability. In particular, we are not sure what about the system changes near the instability that causes something to change with regards to layer sizes. One problem with this graph is we are comparing different timescales. With a different shaking oscillation, our systems characteristic collision times are not directly comparable.

Chapter 5

On Continuous Phase Transitions

5.1 Introduction

Until now, our narrative has been predominately concerned with our investigations into the physics leading to the formation of an instability in our granular fluid. We must ask however, more than just *why* does our system move through this transition, but *how*. From these investigations, and after extensively probing the dynamics of how our system changes from a symmetric state to an asymmetric state, we have found that the spontaneous symmetry breaking in our system bears striking similarities to a variety of interesting physical phenomena, including phase transitions, critical phenomena and universality classes. As might be expected, this change in focus will be accompanied by a change in methodology, with less emphasis being put on a hydrodynamic formulation of physical events and more on a description from a framework more common to nonlinear dynamics.

Various factors have driven our belief that the instability formation we have observed

in our system can accurately be described as a 2nd order phase transition. These include the lack of any apparent hysteretic region (Fig. 5.1), the continuous evolution of the wall velocity between a symmetric and asymmetric velocity profile (Fig. 5.2) and various other similarities to critical phenomena such as diverging time scales (Fig. 5.3) and increased fluctuation sizes (Fig. 5.4).

5.2 Hysteresis...or the lack thereof

Our initial guess as to the behavior of the system was motivated by the sharp transition to an asymmetric state near some critical value of the wall velocity. This ‘jump’ appeared to be similar to a first order (discontinuous) phase transition. To probe this hypothesis more rigorously, we investigated the behavior of the system near the transition point with the expectation that if this was consistent with a discontinuous phase transition, we would expect the system to be hysteretic, i.e. a system whose state depends on its immediate history.

In order to investigate the possible hysteresis of the system, we initialize the system to some wall speed above the known critical threshold and allow the instability to form. At some later time we would then incrementally decrease the wall speed and observe the evolution of the systems mean speed in comparison with data obtained when the system had been started at the new shear rate after being allowed to equilibrate. Any sizable difference between system speeds in the two cases would likely point toward path-dependent behavior in the system. However, as seen in Fig. 5.1, we have always found that a decrease in wall

speeds quickly causes the system to transition to the mean speed that was found had we started the simulation at the decreased speed.

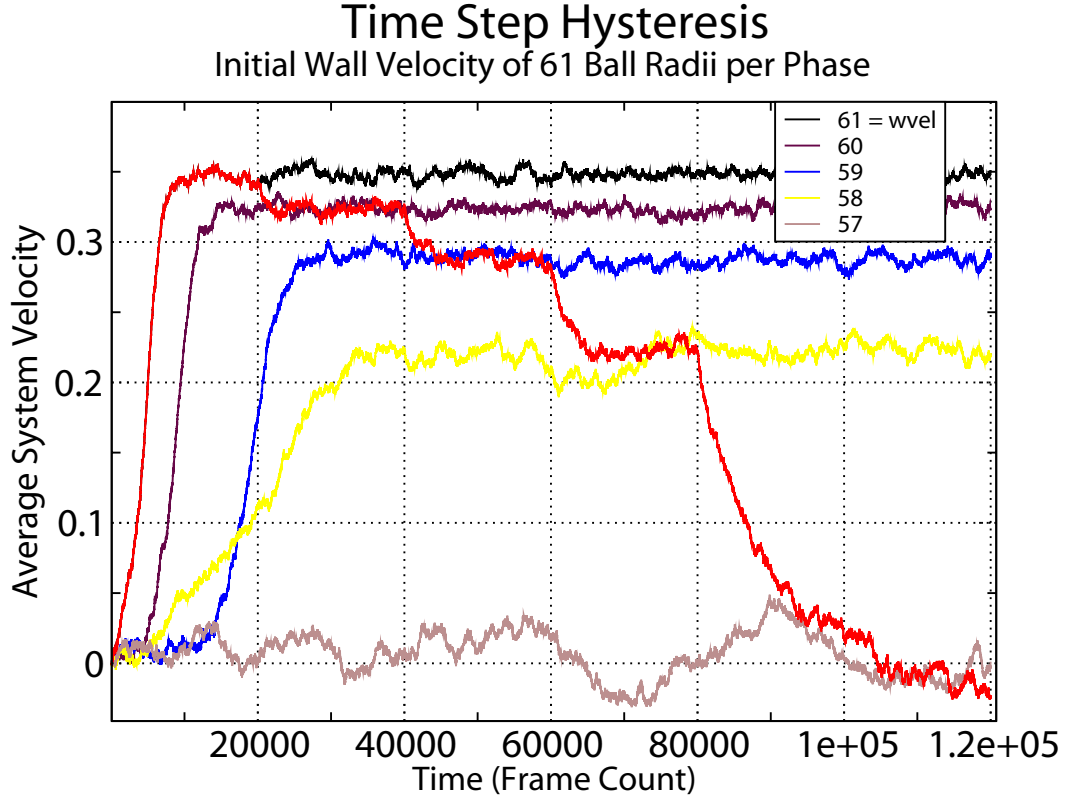


Figure 5.1: Our system is not hysteretic

The black line represents a simulation where every 20,000 frames, the system wall speed is decreased by one ball radii per period. The system average velocity is the arithmetic mean of the y component of the velocities of all the particles in the cell. We only use the y-component because we have found, as discussed in Section 1, that the y-component of the velocity obeys a linear velocity profile that depends only on the x position in the cell. Note that the system regains symmetry at the same value for wall velocity that it is found

to break symmetry at. This is consistent with the existence of a critical point from a second order phase transition. From a nonlinear dynamics perspective, it appears that the system either does not have two stable fixed points, or fluctuations of the velocity of the system are larger than the reversible region. It is therefore reasonable to conclude that the system is not hysteretic, or the region of hysteresis is exceedingly small.

5.3 Continuous Bifurcation

Additional inquiries into the physics of the transition lead us to investigate the evolution of the system mean speed. We would expect a 2nd order phase transition to be characterized by a continuous evolution in the system mean speed as we vary the wall shear rate parameter. Indeed, our measurements of the average system speed, while highly sloped, do appear to be a continuous evolution over a small range of wall velocities.

In Fig. 5.2, data points near the transition point are found by varying the total wall gradient by one ball radii per period. From this graph you can see that there does not appear to be a discontinuous jump in wall velocity over a range of different system sizes, but rather a continuous transition to the asymmetric state. This is particularly interesting from a physical perspective, because it implies that above a critical wall velocity the system is driven continuously farther and farther out of symmetry. Our system appears to have more in common with a girder buckling under pressure than a stick that spontaneously breaks when pressed. From a nonlinear dynamics perspective, this symmetry breaking is referred to as a supercritical pitchfork bifurcation.

Supercritical Bifurcation At .5 density

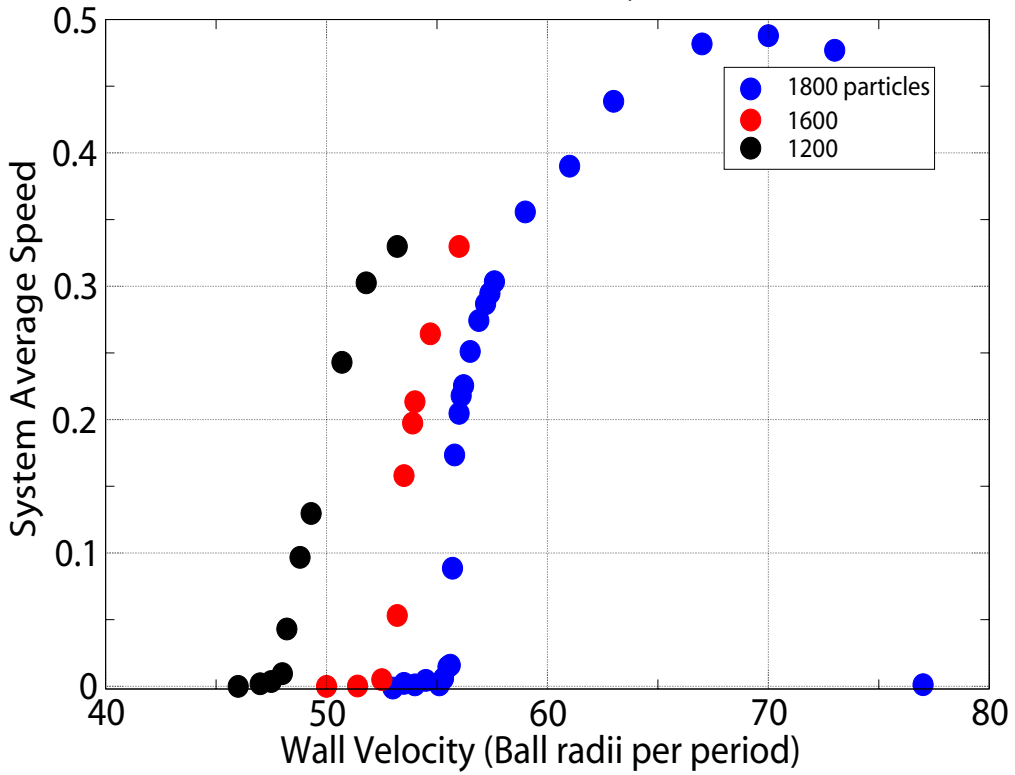


Figure 5.2: System mean velocity bifurcations over a range of system sizes.

Near our possible critical point, the time necessary for the system to reach a steady state increases significantly. Around this region, it becomes difficult to accurately differentiate between large system fluctuations and actual asymmetric solutions to our system. (Fig. 5.3)

As you can see in Fig. 5.3, even over significant timescales (100,000's of oscillations) our simulation does not readily lend itself to perfectly accurate measurements of the transition point. For instance, at a shear rate of 55.7 ball radii per phase (green line above) the system mean velocity is clearly asymmetric for a non-negligible period of time. It could

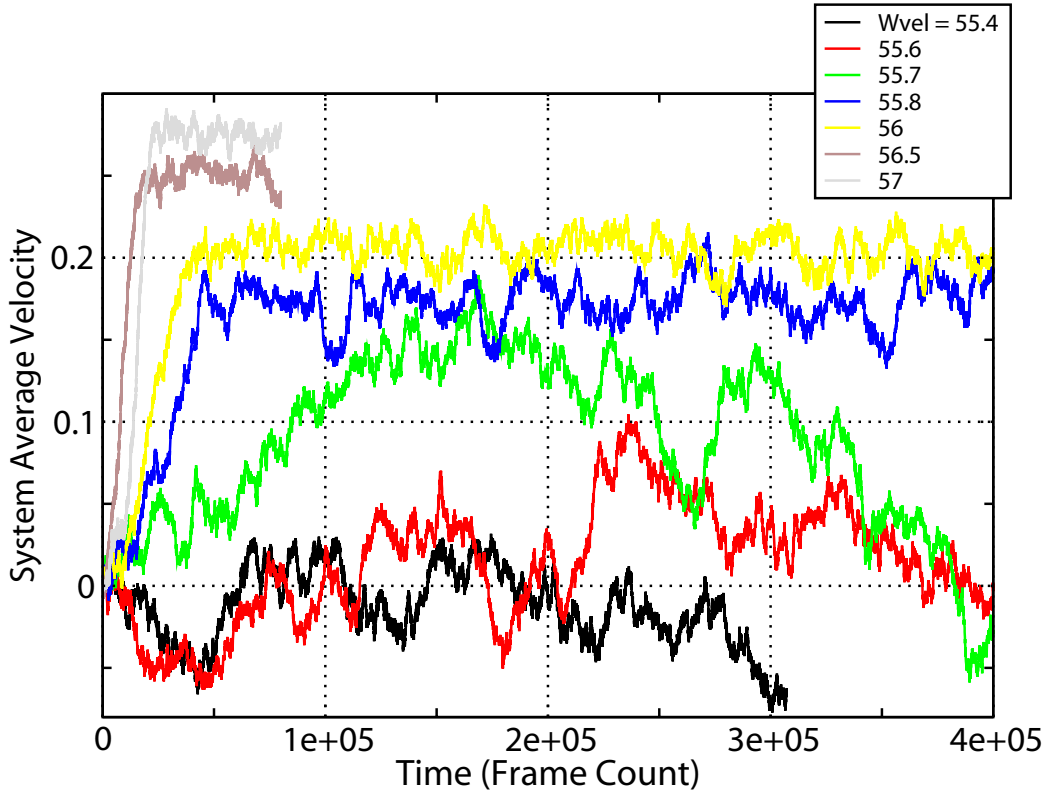


Figure 5.3: Notice the significantly increased time to reach steady state near the critical point

be that this is a large scale fluctuation in the system velocity, but it could also be that the system fluctuations are sufficiently perturbing this state to cause it to transition back to a symmetric state. This implies that without an infinite amount of time to measure our system, we cannot perfectly determine the location of the transition to the asymmetric state. Without a localized position of our critical point, it is difficult to accurately characterize our system with the tools of statistical mechanics. Nevertheless, we can, with a reasonable degree of certainty, describe a range of wall velocities over which we expect the transition

point to lie. It is also important to note that this ‘critical slowing down’ is a signature of 2nd order phase transitions and can be viewed as further evidence that this is in fact what we are seeing in our system.

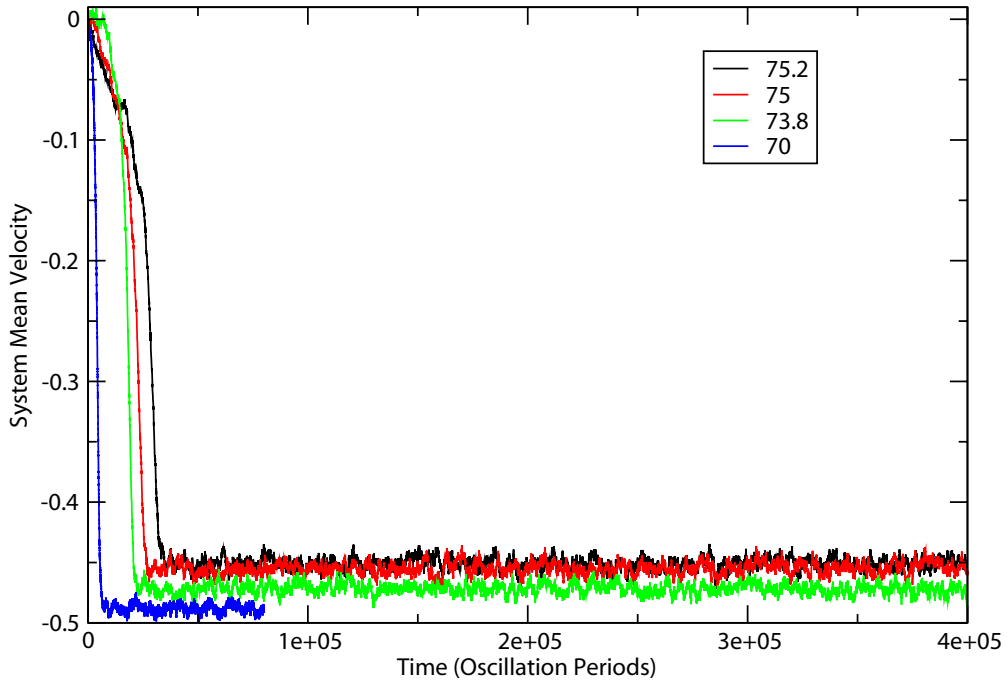


Figure 5.4: Higher wall velocities actually decrease the system mean speed, which is evidence we are approaching the 2nd critical point.

We have not probed the 2nd transition (the point at which the system regains symmetry) as thoroughly. However, our initial investigations have led us to believe that our system is again acting consistent with our basic theories of the dynamics. In particular, we believe that the 2nd transition is similar to the first, in that at some critical wall velocity gradient, the

other wall begins to slip more. The result is that our system falls back into equilibrium with symmetric velocity profiles. Our investigations into the phase transitions of the systems also appears to support this theory, as our system again exhibits critical slowing down as well as continuously bifurcating back to zero. These effects are illustrated in Fig. 5.4, where you can clearly see that as we increase the velocity of the shearing walls, our system reaches an equilibrium mean speed that is lower than it would at lower shear velocities. For instance, the black data points are from a system initialized at 75.2, and the blue line, which is a substantially larger mean system speed, was only at 70. In both systems we can be certain that one wall is slipping substantially, as our system has undergone a transition to the asymmetric state. However, it appears likely that the slip at the other wall is growing substantial enough to lower the mean system speed. In addition, you can see that the higher wall speed systems are taking longer to evolve to the asymmetric state, which is likely a result of critical slowing down as we near the 2nd critical point.

5.4 Critical Phenomena

If the bifurcation is consistent with a continuous phase transition, there are a variety of effects we expect to see, such as diverging correlation lengths, critical exponents and other indications of universality.

Our attempts to exactly classify the location of the critical point is made more difficult by the fact that the system stability is lower near the critical point, and the system becomes more sensitive to small perturbations. In fact, a cursory look at Fig. 5.5 below indicates that

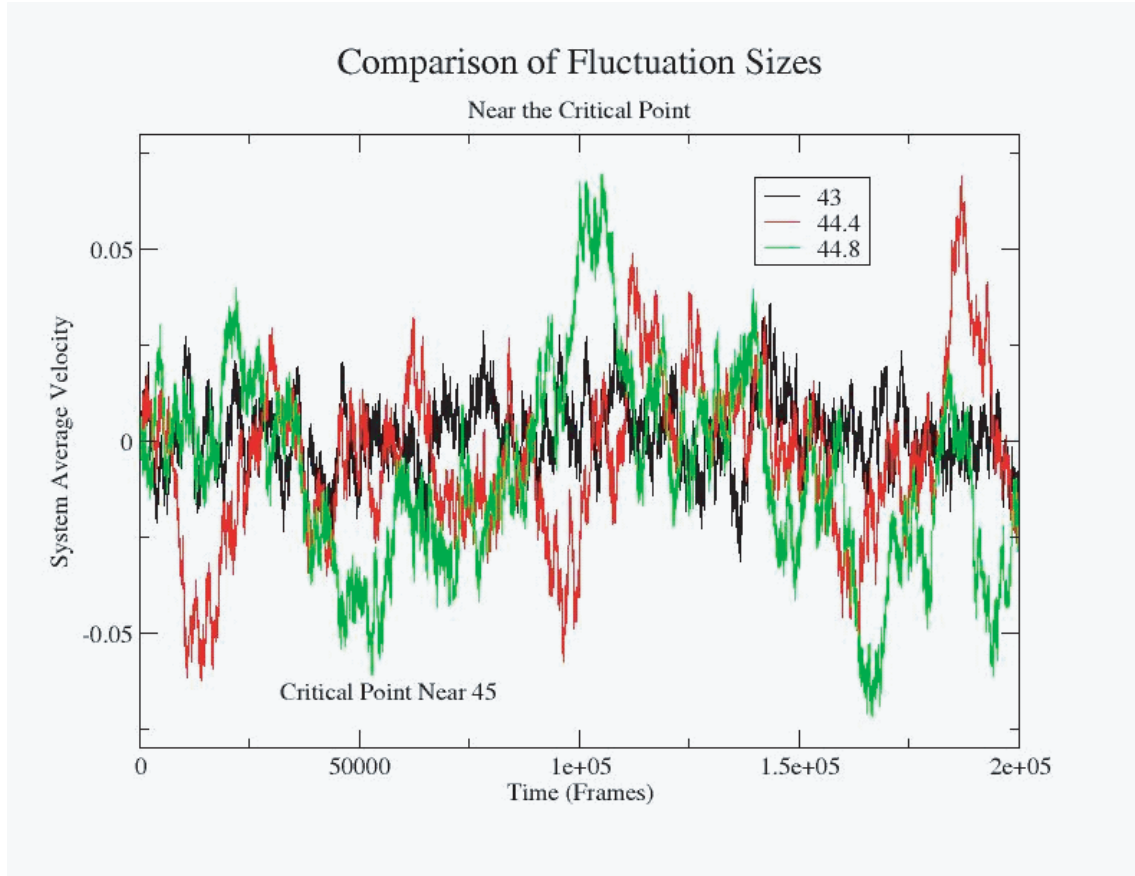


Figure 5.5: A comparison of fluctuation sizes and timescales near the critical point

as the velocity of the shearing walls is increased, fluctuations in the system average velocity become larger and more frequent. Additionally, we expect that the system fluctuation sizes become increasingly non-Gaussian near the critical point, because of a divergence in the correlation lengths at this point[15].

Here, the black line has significantly smaller fluctuations. We say this because the fluctuations have significantly greater magnitude as the system parameter is adjusted towards the critical point. A more precise way to prove this is by measuring the size of the mean square fluctuations, which is equivalent to the statistical variance of the system average

velocity $\langle V \rangle$. This calculation is relatively straightforward, as the variance is equal to the expectation value (mean value) of the system average velocity squared minus the squared expectation value of the system average velocity:

$$\text{var}(v) = \langle V^2 \rangle - \langle V \rangle^2$$

We can calculate these parameters rather efficiently in our code by simply keeping velocity values as we run our code:

$$\begin{aligned}\langle V^2 \rangle &= \frac{1}{N} \sum_{i=0}^N (V_i^2 - V_{\text{average}}^2)^2 \\ \langle V \rangle &= \frac{1}{N} \sum_{i=0}^N (V_i - V_{\text{average}})^2\end{aligned}$$

Here, N is the number of particles used in the simulation, and V_{average} is just the arithmetic mean of the particle velocities:

$$V_{\text{average}} = \frac{1}{N} \sum_{i=0}^N V_i$$

Note that all the velocities being considered are exclusively the y-component of velocity, because as stated in Section 1, the y-component of velocity is what breaks symmetry.

In Fig. 5.6, one can visibly understand that the fluctuation sizes nonlinearly increase near the critical point for a variety of system sizes. In fact, for points closest to the transition, the variance of the system velocity is significantly larger than the system mean speed after we believe it bifurcates. As a result, the velocity profiles begin to look like they are breaking symmetry over short timescales, when in reality we believe these are just large system-wide fluctuations.

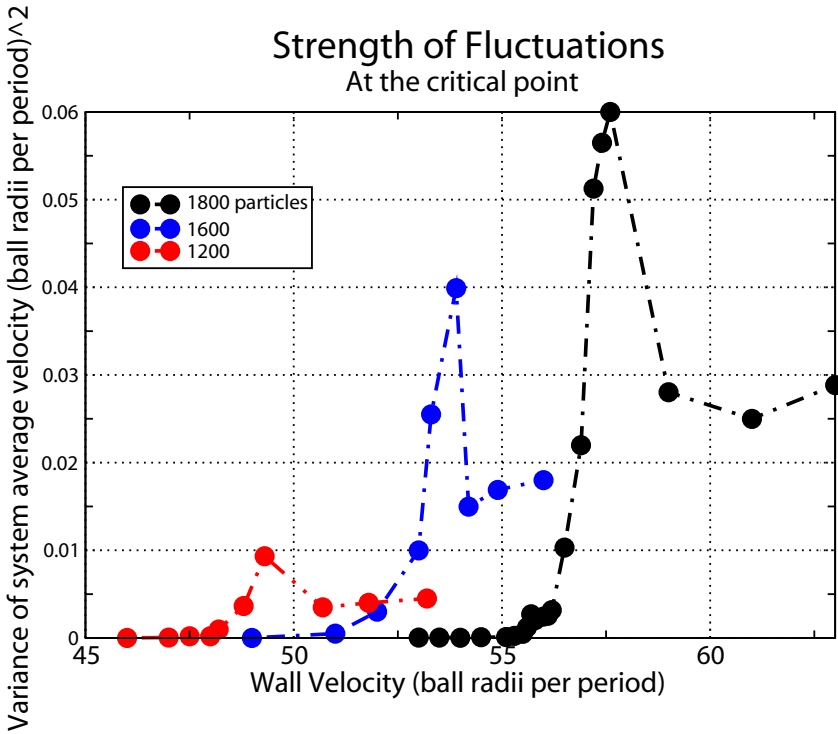


Figure 5.6: The strength of system fluctuations grows as we approach the critical point, which is common in 2nd order transitions

Additionally, we do not believe that one should pay close attention to the fluctuation sizes far from the transition because, as stated previously, the system has a 2nd transition that occurs shortly after the 1st. As we believe these transitions are generated by the same phenomena (the wall beginning to slip) we would then expect that the system is again nearing a transition point, and with it, large scale system fluctuations. Therefore, the fact that the variance does not drop down greatly at this point is likely caused by the 2nd transitions fluctuations becoming non-trivial.

5.5 Discussion

By finding some basic relationships to equilibrium statistical mechanics, our system is suggestively pulling us toward an enormous realm of possible results and correlations with classical thermodynamic systems. At this time we do not conclusively know if there are more concrete and meaningful connections to make with more traditional equilibrium systems, but the possibility of doing so is tempting, as any rigorous connection would be a significant result.

The most obvious connection would likely be following a path akin to that of Miller and Huse[16], where a chaotic map was found to possess an ordered phase like that of a two dimensional Ising system. In fact, our system appears to have several similarities to the Ising model, especially if one regards the symmetry breaking as a ferromagnetic transition of spin states. In effect, we would be regarding the broken symmetry of our system as a collection of ‘up’ or ‘down’ spin sites. Clearly this is not a perfect analogy, as while spin is intrinsically quantized in the Ising model, the magnitude of particle velocities in our system are not.

The most obvious path to proving a connection between our system and the Ising model more rigorously would be to measure several of the critical exponents of our system. This would be most easily realized by finding power law behavior in graphs similar to Fig. 5.6. However, we are not yet confident enough in the location of the critical point of our bifurcation curves to have confidence in assigning our system a particular critical exponent for this transition. To accurately characterize the transition, we would require accurate data for

several other critical exponents. If this was accomplished, we would quite possibly be able to assign our system to a particular universality class. This would be tremendously useful, as a universality class bands together systems that have the same critical behavior. While this characterization remains elusive, and even speculative, it is not outside the realm of possibility and so bears mention here.

Chapter 6

Conclusions

In this thesis we have attempted to introduce the reader to our simulation and the process we have undergone with regards to classifying its dynamics. In particular, we have been focused on advancing our knowledge of this system in two directions. Our primary objective has been to judge the accuracy of hydrodynamic descriptions when applied to granular flows. Additionally, we have sought to accurately model, characterize and predict the dynamics of the symmetry breaking we observe in our system.

As stated previously, much of our emphasis has been to investigate the applicability of fluid dynamics to granular flows. We have shown that there are several notable instances in which relations more common to hydrodynamics provide at least a rudimentary description of the kinematics of our system. The existence of linear velocity profiles, the direct proportionality between system width and instability formation as well and the existence of boundary layers consistent with the structure we would expect in a rarefied gas are all evidence that there are strong connections to be made between granular and fluid flows.

Additionally, we have probed the dynamics of the transition itself, and found several significant results. The transition to an asymmetric state is not a discontinuous jump, but a continuous, smooth transition from symmetry. The critical slowing down, fluctuation sizes and finite size effects are all characteristics commonly associated with 2nd order phase transitions. These results point toward connections between this nonequilibrium system and classical statistical mechanics.

There is much more work that could be done on this subject. Additional work is needed on finding the strength of the correlation between the realm of fluid dynamics and granular media. In particular, it could be interesting to probe the dynamics at the layers much more intensively. While these layers were certainly considered in the course of this study, they were not the focus. Based on their anomalous behaviour at different frequencies of shaking as well as near the instability, we believe that the small boundary layers could be a major force in driving the system to an asymmetric state.

In addition, more detailed investigations need to be opened on the phase transition. How closely does our non-equilibrium granular flow follow classical systems like the Ising model? This could be probed by actual measurements of the correlation lengths or critical exponents.

While this remains a work in progress, it is our hope that we have continued to lay a foundation for one day providing a comprehensive theory of granular flows, or perhaps even the nonequilibrium sciences in general. No comprehensive theory yet exists, but, when it does, it will quite possibly take a familiar form as an extension of another subset of physics. Other research has found interesting connections between far from equilibrium

systems, statistical mechanics and hydrodynamic instabilities[4, 5, 17]. Our work could be suggesting that we add granular flows to that list.

Appendix A

The Experimental Setup

Our computation simulation is based on an experimental apparatus that was in Professor Urbach's lab. As can be seen in Fig. A.1, the system is a round plate with small ball bearings. It is radially symmetric, and has dimensions of approximately $r = 45$ cm and height approximately 2.7 mm. The disk is placed on top of a shaker, which can run over a wide range of frequencies of oscillation. The inner disk is capable of running at least at several hundred RPM, with typical speeds in the experiment much lower.

The data was collected by a Pulnix TM1040 camera, with typical frame rates around 10 microseconds. A typical picture is shown in Fig. A.2.

Obviously, the circular apparatus greatly differs from our rectangular cell size in the computational simulation. In addition, the shear of the middle plate does not impart nearly as significant an impact on our grains in the physical system, and so we have been unable as of yet to reproduce the symmetry breaking state. This is predominantly because friction is significant, a quantity we neglect altogether in our simulation on the computer. More

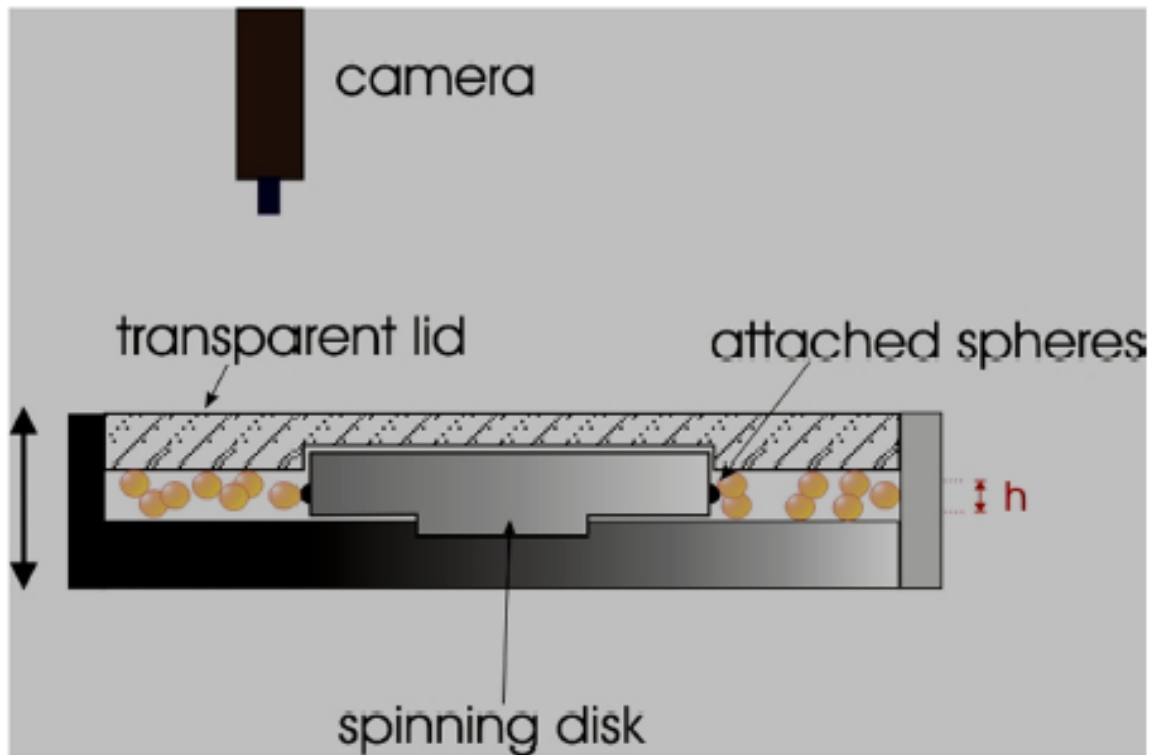


Figure A.1: A side view of the experimental setup

work was done on this previously[8, 14] and will not be reproduced here, needless to say, we do find agreement between our simulation with friction and the experiment. More experimental work would therefore be worthy of investigation in an attempt to find an instability like which has been presented in our paper.

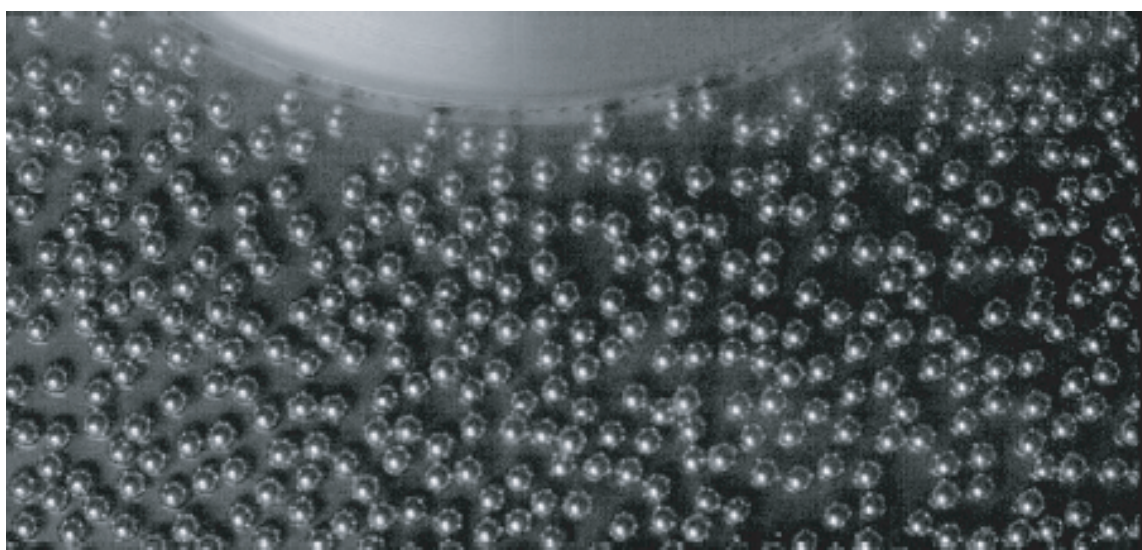


Figure A.2: A snapshot of the experiment

Appendix B

Comparison with other systems

With any computational simulation, one cannot be sure that the results of the simulation will correspond to physical systems due to the assumptions implicit to running the model. It is therefore important to seek similarities with known affects or familiar systems to increase the confidence one can put in the measurements from the simulation. For our particular system, we have found a variety of instances that leads us to believe that what are seeing in our simulation has a applicability to other models, and reality as a whole. We were initially recommended to seek out shear bands[18], which lead us to turning off the shaking in our system. From this we found that while no bands formed, the bulk of our granular system settled down to the middle of the system, which is clearly illustrated in the pictures below. In particular, our density profiles imply that most of the bulk is in the middle, and the velocity profiles are less steep, and suggest that most of the media is moving very slowly. These profiles have enough in common with other works[22] that we have enough confidence in our system dynamics to believe our symmetry breaking

represents a novel effect that bears more research.

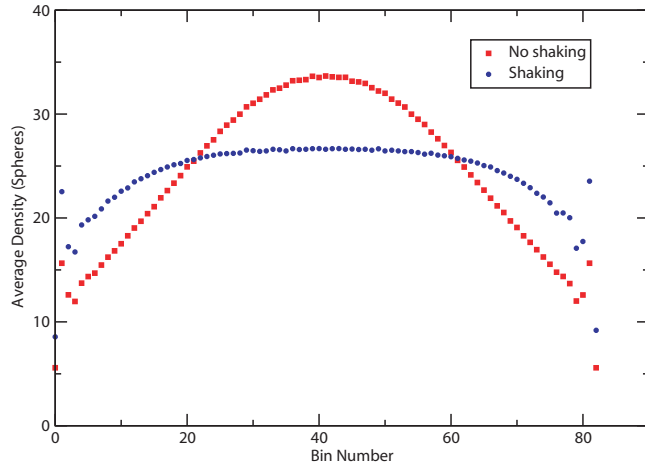


Figure B.1: A comparison between density profiles with and without shaking.

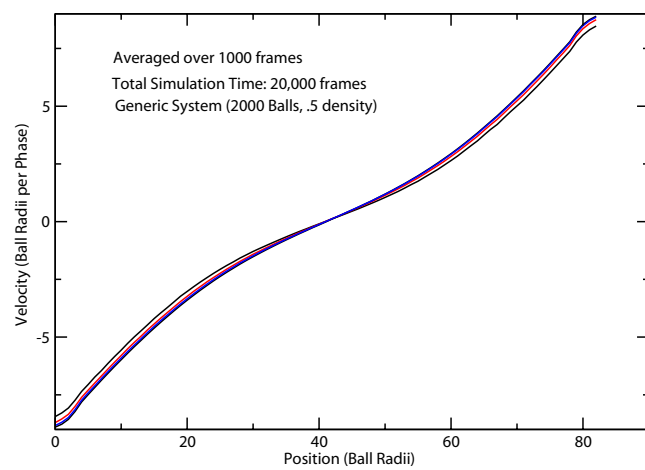


Figure B.2: A velocity profile for a system with no shaking. Notice the lack of linear profiles

Appendix C

Fruitless Pursuits

Any sufficiently rigorous investigation into a non-trivial physical system is almost certainly bound to lead to dead ends. This project most certainly had its share of intractable problems crop up. At the same time, mistakes and missteps can be almost as useful as advances for those continuing a project for it provides insight into some of the more complex and challenging problems faced. This section is my attempt to introduce the reader to several of the problems I was unable to overcome in the course of my research.

C.1 Mean Free Path

By far the most significant portion of my work that is not contained in the main text pertains to computations of the system mean free path. As discussed in the text, we have been constantly puzzled by the dynamics of the boundary layers. It is quite possible that a better understanding of the activity at the boundary layers would shed light on the system

dynamics as a whole. We were thus prompted to investigate the dynamics of these layers from the perspective of other systems that possess similar structure. As rarefied gases posses similar layers, it seemed natural to attempt to extend our work on describing our system as a fluid to one with a medium sized Knudson number (I am not sure how to pronounce it either). The Knudson number (Kn) is a parameter which relates the ratio of the system mean free path (λ) to the characteristic length of the system. It may take any non-zero number, and so the magnitude of the number can be useful for characterizing the expected fluid dynamics of the system. In other words,

$$\text{Kn} = \frac{\lambda}{l}$$

Intuitively, we can expect a Knudson number that is nonzero, but certainly not enormous. This is because our system mean free path is visible by watching the movies of the particles, and balls can be seen moving for several time steps between collisions. Furthermore, our system width is several times the length of a ball diameter, but certainly does not dwarf our estimated mean free path.

A typical fluid will have Kn that tends to zero. These are the most commonly discussed fluids, and conform almost perfectly to the no slip conditions. At the other end of the spectrum, there are systems with very high Kn . This corresponds to extremely rarefied gases and is often called ‘free molecular flow’[13]. We do not expect this to be appropriate for our system, as at these scales the gas is considered sufficiently rarefied as to neglect all particle interactions, and only discuss the interactions with the boundary (in our case it would be the shearing walls). Anyone who views a video of the system will notice that there are numerous interactions between particles. In fact, the part of the mean free path

code that did work implied that there were orders of magnitude more collisions between particles than with the walls. For fluids with small, but still nonzero Kn, we expect to find a boundary layer between the fluid and the system boundary. In this regime, Kn is on the order of the mean free path, which is certainly possible for our boundary layer size, which was on the order of several ball radii. We expect this is the regime in our system.

The boundary layer is a ‘slip layer’ where the velocity profile jumps between the bulk velocity and temperature toward the conditions at the boundary. Even with this change, we would expect that the layer will generally not perfectly with the velocity at the shear wall. If our system is actually within this region, we would expect that the velocity jump at this layer would be proportional to the change in the velocity profile times the mean free path:

$$\Delta V \propto \frac{dV}{dy} \lambda$$

In order to test this relation, we need a method to calculate the mean free path.

We have investigated several ways to calculate the mean free path of our granular system. Our simplest method was to estimate the mean free path from the density using the Boltzman Collision Frequency[19]:

$$\omega_0(T) = 2\pi n \sigma \sqrt{\frac{T}{\pi m}}$$

where σ is the dimension of our object, T the temperature, m the mass (which is just one in our dimensionless formulation) and n is the density. Our only problem with using this formulation is that our system is quasi-two dimensional. So while the balls are moving in three dimensions, they are constrained to a monolayer. From this equation we can estimate a collision frequency of approximately 5 collisions per phase. While this is on the order

of what we would expect, it is difficult to accurately measure this. In addition, we cannot effectively separate the effect of the temperature and shaking from our temperature in our calculation of the mean free path. As a result, we implemented a direct collecting of the mean free path in our system.

Mean free path is simply the average distance between collisions. We are interested in the dynamics of the mean free path near the boundary layers, and so it is important that we again break our results into bins that are divided between the shearing plates.

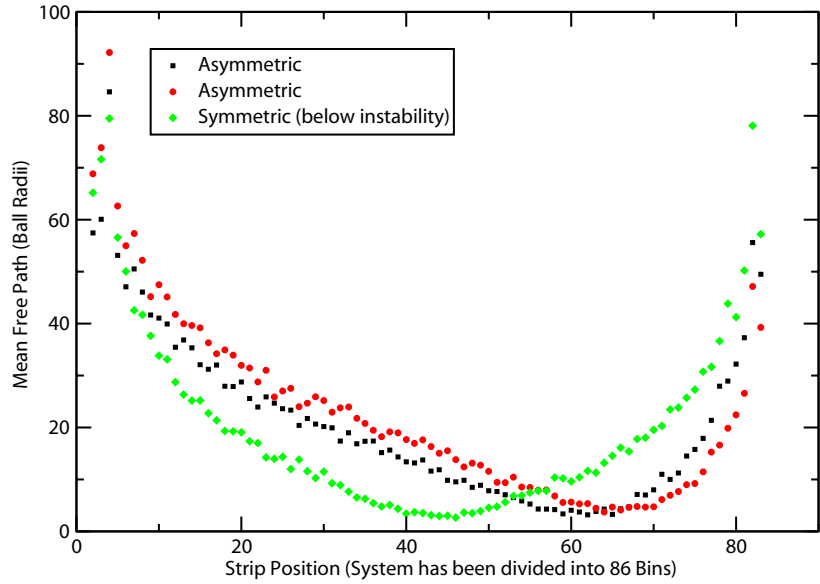


Figure C.1: The system mean free path. Notice we find an asymmetry in the profile.

We find that the collision frequency around the middle is approximately 3.7 collisions per period, which is on the order predicted by our collision frequency. In addition, we observe a broken symmetry when the system is brought into the asymmetric state. While

these results are intuitively correct, our mean free paths are far too high along the edges. We concluded that we additionally needed to calculate the mean free path with the x-velocity as the local flow, since while the edges are moving more quickly, they are not moving much faster locally, given the speed of the wall and surrounding granular fluid.

We modified our calculations of mean free path by subtracting out the average distance traveled by a particle in the local area. Note that we are approximating our system to be 2 dimensional, since the distance traveled in the z-direction should be negligible:

$$\lambda = \frac{1}{n} \sum_{i=0} n \left[(\Delta x - v_{\text{strip}} \Delta t)^2 + (\Delta y)^2 \right]^{1/2}$$

However, it is here that our work dies out. The mean free path program that was written never really worked, which is unfortunate because it is possible this could have shed light onto how our layers were acting. Basic approximations about the dynamics did not give strong results, and it is possible that one of our assumptions about kinetic theory does not hold in granular systems. It is our belief that this is a possible track to accurately describing the system, but unfortunately, we do not yet have the data to back that assertion up.

C.2 Other Paths Investigated

We investigated several other interesting elements in our system that we were regrettably unable to completely investigate. Several of these elements are not well investigated, but it bears mention here for the sake of completeness.

As discussed in Section 3.4, we see anomalous structure forming along the edges of our layers. In particular, some of the bins along the edges have a significantly greater

amount of particles in them, on average. It seems logical to investigate this further, because any structure forming in such a location could tell us more about the layers. Our original approach to this was to plan on implementing an autocorrelation as a function of position. In particular, this could be accomplished by using the Wiener-Khinchin Theorem[20].

We also looked at the velocity distributions of our system. As we near the transition point, the variance of the system grows (as we have discussed before) and so corresponds to a wider distribution. Additionally, it appears that the distribution becomes less and less Gaussian as we near the transition point. This could point toward various assumptions from kinetic theory such as molecular chaos, etc. increasingly breaking down at higher temperatures. However, we do not have a strong hypothesis about why this is happening.

Finally, one of our collaborators, Professor Isaac Goldhirsh of Tel-Aviv University, who in addition to working with us on the mean free path mentioned earlier, pointed us toward investigating if our balls were possibly ‘double bouncing’ or hitting the same wall twice before hitting anything else. It appears that this did happen, and we are not entirely sure why. The frequencies measured for these events are extremely low, with approximately 0.004% of all collisions taking place in this manner. It does not appear that this occurs any more frequently on either wall, or after the instability has formed. On the other hand, because they are so rare, we do not have large amounts of statistics about these events, and so it is possible that with more data there could be interesting physics behind the events.

Appendix D

The Parameter Space Sampled

We have a strong understanding of the conditions under which our instability sets in, which has formed the basis for our theories as to why the system transitions to an asymmetric state. However, we are still trying to probe the parameter space to come to a full understanding of precisely what mechanisms are dominating the system, especially with regards to anything that could be linked to well understood physics. In effect, this section serves to place some of the data I collected during my research that I did not feel has a place in the main text.

One avenue we have investigated is the dependence on the system density to the formation of an instability. I had hoped to map this out more fully and even put together a ‘phase diagram’ for the system dependence on wall velocity, density, etc. Unfortunately I did not have time to really map out this space. Our most basic intuition, that the system will break symmetry at lower speeds for higher densities, is correct. For instance, a system that is initialized to .5 density with 1600 particles at ‘typical’ parameter values ($g = 1$, shaking frequency $\nu = 50$, etc.) will break symmetry at approximately 55.5 (higher) ball radii, but

for a system of 1600 particles at .55 density, the speed will be 54.2. This is likely a result of the system width shrinking for lower densities.

The variance increases as a function of time, continues to grow as the system is driven out of symmetry, and then abruptly collapses when the system reaches steady state. This data is not contained within because I must intrinsically quantize the intervals I look over, and I was not confident that this did not introduce some fundamental error into my analysis. Nevertheless, it was an interesting result, as I would perhaps have expected the fluctuation sizes to decrease as the system was driven through the asymmetric trajectory. This appears to support the idea that our system is being driven out of equilibrium by large system fluctuations that occur.

Some Interesting Parameter Sets: (Unless I specifically state so, assume most of the parameters are ‘typical’)

At 2000 particles, the first instability is around 57 (I found 57.6, but as I said before, I am not confident that this is perfectly correct), and the 2nd instability is near 75.

For 1171 particles, at a system size of $40 L_x$ and $212 L_y$, the instability is around 44.9.

Likewise, for 1268 particles with $50 L_x$ and $182 L_y$, the system broke symmetry at 47.

The 2nd instability *does not occur* at an equal distance from the 1st for all parameter sets. Nor really, should we expect it to. It does however, appear to scale with the system size (larger system implies greater distance between instabilities) but I did not investigate this further.

For a system of 1268 particles with NU at 25, the symmetry is broken at approximately 85 ball radii.

At NU of 75, the symmetry breaks at 35.5

For those interested in a closer look at this data, I have put all the graphs of my thesis, along with this document itself, on my home directory on *Fire*.

Additionally, a complete compilation of my work this last year is on DVD in the possession of Professor Urbach, so I am sure you could fight him for it.

Bibliography

- [1] D. Howell, R.P. Behringer, and C. Veje. Stress fluctuations in a 2D granular Couette experiment: A continuous transition. *Phys. Rev. Lett.* **82**:5241 (1999).
- [2] P. Bak, C. Tang, and K. Wiesenfeld. Self-organized criticality: An explanation of the 1/f noise. *Phys. Rev. Lett.* **59**:381 (1987).
- [3] Several of these interesting results are described in: A. Prevost, D.A. Egolf, and J.S. Urbach. Forcing and velocity correlations in a vibrated granular layer. *Phys. Rev. Lett.* **89**:084301 (2002). In addition, this system should have a variety of similarities with our system.
- [4] J.P. Gollub. Order and disorder in fluid motion. *Proc. Nat. Acad. Sci. USA* **92**:6705 (1995).
- [5] D.A. Egolf. Equilibrium regained: From nonequilibrium chaos to statistical mechanics. *Science* **287**:101 (2000).
- [6] Of which a terrestrial based experiment is still exclusive to science fiction, and actual experiments outside the Earth's atmosphere are prohibitively expensive. This might

seem to be a minor point, but some of the funding for this grant is actually directed to investigating granular dynamics in a microgravity environment. Perhaps the greatest change to our system dynamics is that we have 'turned off' the friction between the top and bottom plates.

- [7] Such as: X. Nie, E. Ben-Naim, and S.Y. Chen. Dynamics of vibrated granular monolayers. *Europhys. Lett.* **51**:679 (2000).
- [8] J. Cameron Booth. *Non-equilibrium dynamics in excited granular media*. Senior thesis at Georgetown University, Department of Physics, 2005.
- [9] A. Sommerfield. *Thermodynamics and statistical mechanics*. Academic Press, New York, 1965.
- [10] D.J. Tritton. *Physical Fluid Dynamics*. Oxford University Press, New York, 1988.
- [11] A substantial derivation of the Navier-Stokes equations begins with the conservation of mass, momentum, and energy for a finite-volume. It is effectively a formulation of Newton's second law in a continuum.
- [12] The no slip condition is the typical continuous hydrodynamic assumption that the velocity and temperature of the gas is equal to the velocity and temperature of the wall. The existence of boundary layers clearly leads us to conclude our system does not obey such a condition.
- [13] M. Kogan. *Rarefied gas dynamics*. Plenum Press, New York, 1969.

- [14] P. Kumar. *Shaken and sheared granular flows*. Senior thesis at Georgetown University, Department of Physics, 2006.
- [15] M.C. Cross and P.C. Hohenberg. Pattern-formation outside of equilibrium. *Rev. Mod. Phys.* **65**:940 (1993).
- [16] J. Miller and D.A. Huse. Macroscopic equilibrium from microscopic irreversibility in a chaotic coupled-map lattice. *Phys. Rev. E* **48**:2528 (1993).
- [17] S.T. Bramwell, P.C. Holdsworth, and J.F. Pinton. Universality of rare fluctuations in turbulence and critical phenomena. *Nature* **396**:552 (1998).
- [18] W. Losert, personal communication at Dynamics Days 2007, Boston, Mass.
- [19] Pagonbarrage, et al. *Randomly driven granular fluids*. *Phys. Rev. E* /bf 59:4326 (1999).
- [20] This is accomplished by performing a Fourier transform on the position of the particles, and squaring the transformed data before returning to normal space (inverse Fourier transform).
- [21] Our systems actual width is actually slightly larger than the value given, because there are small gaps along the walls. These gaps are a result of our walls not being perfectly flat surfaces, but are rather made up of a series of rigid balls all packed next to each other. Therefore, some extra area exists between each of the balls that is not being reflected in our data. A larger area would imply that even at the intercept on the graph, the system has some nonzero area.

- [22] Sundaresan, et al. *The effects of boundaries on the plane Couette flow of granular materials: a bifurcation analysis*. J. Fluid Mech. **397**:203 (1999).
- [23] Wigner, Eugene. *The Unreasonable Effectiveness of Mathematics in the Natural Sciences*. Communications in Pure and Applied Mathematics. **13**:1 (1960).

Acknowledgments

Before I started my research, I purchased two books: Ott and Tritton (both cited in this work), which at the time I largely did not understand. At the end of August, I revisited these texts and found, to my great surprise, that an enormous deal of the content was now well understood to me. In short, this senior year research project has been the greatest learning experience of my life. I have come to grips with extremely advanced concepts in the sciences and have even been able to personally contribute to some of these subjects.

Probably the greatest boon of undertaking this project has been the guidance of my advisors, Professors Jeffrey Urbach and David Egolf, as this has allowed me to see how professional scientists think about and approach a problem. This work has served to truly cement my personal belief that I am interested in pursuing a career in the sciences, and has inspired me to continue my education in graduate studies, with the hope of eventually earning the distinction of being conferred a doctorate. More importantly, I felt that whenever I worked, they were more than willing to meet me halfway (far more than that!) and help me along. I am proud to say I feel that I have earned some respect in the eyes of two individuals I cannot respect more.

Professor Egolf constantly went above and beyond the call of duty, going so far as to shoot me down when I gave my presentation to him for the third time at 1:00 AM the

morning I was suppose to give my final thesis talk to the faculty. The criticism worked: I stayed up late, made some serious revisions, and then nailed the presentation.

In addition, I would like to especially thank my direct predecessor, Pramukta Kumar, for his help and continued interest the project. This significantly increased the speed at which I was able to start this project.

I would additionally like to thank everyone else in the Physics Department at Georgetown University, all of whom have greatly contributed to my enjoyment and success these last four years. I will leave with only fond memories and Georgetown always in my heart.

I do sincerely hope that some of the questions that have arisen from this project will be investigated by another inquisitive individual, and I wish them best of luck!

This work was supported by: **National Science Foundation grant DMR-0094178**
NASA grant NNC04GA63G